JB
Journals.ASM.org

The Highly Conserved MraZ Protein Is a Transcriptional Regulator in *Escherichia coli*

Jesus M. Eraso,[a] Lye M. Markillie,[b] Hugh D. Mitchell,[b] Ronald C. Taylor,[b] Galya Orr,[b] William Margolin[a]

Department of Microbiology & Molecular Genetics, University of Texas Medical School at Houston, Houston, Texas, USA[a]; Environmental Molecular Sciences Laboratory and Fundamental & Computational Sciences Directorate, Pacific Northwest National Laboratory, Richland, Washington, USA[b]

The *mraZ* and *mraW* genes are highly conserved in bacteria, both in sequence and in their position at the head of the division and cell wall (*dcw*) gene cluster. Located directly upstream of the *mraZ* gene, the P_{mra} promoter drives the transcription of *mraZ* and *mraW*, as well as many essential cell division and cell wall genes, but no regulator of P_{mra} has been found to date. Although MraZ has structural similarity to the AbrB transition state regulator and the MazE antitoxin and MraW is known to methylate the 16S rRNA, *mraZ* and *mraW* null mutants have no detectable phenotypes. Here we show that overproduction of *Escherichia coli* MraZ inhibited cell division and was lethal in rich medium at high induction levels and in minimal medium at low induction levels. Co-overproduction of MraW suppressed MraZ toxicity, and loss of MraW enhanced MraZ toxicity, suggesting that MraZ and MraW have antagonistic functions. MraZ-green fluorescent protein localized to the nucleoid, suggesting that it binds DNA. Consistent with this idea, purified MraZ directly bound a region of DNA containing three direct repeats between P_{mra} and the *mraZ* gene. Excess MraZ reduced the expression of an *mraZ-lacZ* reporter, suggesting that MraZ acts as a repressor of P_{mra}, whereas a DNA-binding mutant form of MraZ failed to repress expression. Transcriptome sequencing (RNA-seq) analysis suggested that MraZ also regulates the expression of genes outside the *dcw* cluster. In support of this, purified MraZ could directly bind to a putative operator site upstream of *mioC*, one of the repressed genes identified by RNA-seq.

Escherichia coli varies the timing of cell division, DNA replication, and peptidoglycan (PG) synthesis, depending on the phase of growth, nutrient availability, and the respiratory or fermentative mode of growth (1–5). An ~17.8-kb region located at approximately min 2 on the *E. coli* chromosome, called the division and cell wall (*dcw*) cluster, consists of 16 genes expressed in the same orientation that are involved in the biosynthesis of PG and assembly of the cell division apparatus, also called the divisome (Fig. 1A). This cluster is highly conserved in prokaryotes in terms of both gene content and gene order (6–8).

The *mraZ* (*yabB*) and *mraW* (*yabC*, *rsmH*) genes, which are usually the first two genes in the *dcw* cluster in many bacterial species, are no exception in terms of conservation (9, 10) (see Tables S2 and S3 in the supplemental material). Because of the specific location of their genes, it has been assumed that the MraZ and MraW proteins might have functions related to cell division and PG synthesis (7, 11, 12). Nonetheless, their presence in mycoplasmas (13), which usually lack cell walls, is suggestive of additional and/or alternative functions. Considering their conservation, knowledge about their functions is relatively limited. The N-terminal end of MraZ, encompassing approximately 45 residues, is similar to the N-terminal DNA-binding domains of the transition state regulator AbrB from *Bacillus subtilis* (14, 15) and the antidote protein of the MazE/F addiction module, MazE, from *E. coli* (16). AbrB and MazE are members of a family of transcriptional regulators that have a dimeric N-terminal region consisting of a four-stranded β sheet and a C-terminal DNA-binding domain forged from one α helix and a looped hinge, constituting a so-called "looped-hinge helix fold." It has been proposed for AbrB that this looped-hinge helix motif reorients with respect to the four-stranded β-sheet, allowing a localized induced fit between the protein and DNA target sites. This, in turn, would allow AbrB to bind unrelated DNA sequences with high specificity and affinity. This DNA recognition fold is present in bacteria and archaea (17). Because of the similarity at their N-terminal ends, AbrB, MazE, and MraZ had been grouped into a superfamily of proteins, and by inference, it had been suggested previously that MraZ might also bind to DNA (14).

MraZ from *E. coli* ($MraZ_{Ec}$) and *Mycoplasma pneumoniae* ($MraZ_{Mp}$), which share 28% sequence identity, have both been crystallized (6, 18), and the solved structures are unusual. MraZ contains two tandem homologous copies of the UPF0040 fold, a novel protein fold with no significant similarity to any other proteins whose three-dimensional structures are known (19). Furthermore, both proteins have a tendency to multimerize; $MraZ_{Ec}$ oligomerizes as a dodecamer, whereas $MraZ_{Mp}$ assembles as an octamer. Both oligomers adopt a toroidal structure.

MraW, one of 21 16S rRNA methyltransferases (MTs) present in *E. coli* (20), methylates 16S rRNA at position C1402 *in vitro* in an *S*-adenosyl-L-methionine (AdoMet)-dependent manner (21). Interestingly, MraW might also use proteins as substrates for methylation. Two unknown proteins of 20 and 60 kDa were methylated when MraW was overproduced *in vivo* (22), although this may reflect either direct or indirect methylation. Similar to other AdoMet-dependent MTs, MraW releases *S*-adenosyl-L-homocysteine as a methylation by-product. The structure of MraW is also unusual. Conserved amino- and carboxy-terminal domains of MraW form the MT fold, as well as an internal, approximately

Received 19 November 2013 **Accepted** 19 March 2014
Published ahead of print 21 March 2014
Address correspondence to William Margolin, william.margolin@uth.tmc.edu.
Supplemental material for this article may be found at http://dx.doi.org/10.1128/JB.01370-13.

doi:10.1128/JB.01370-13

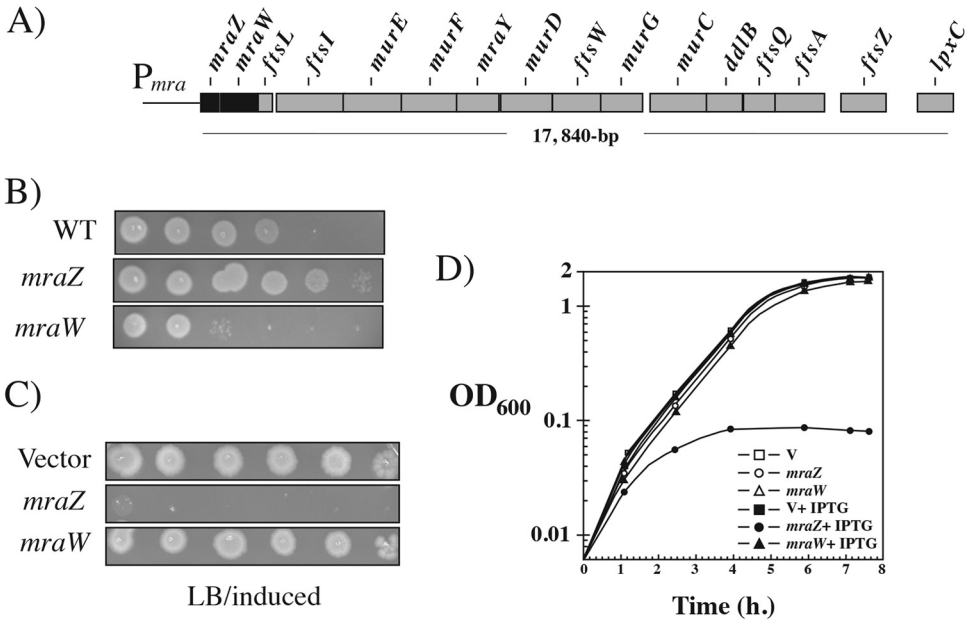

FIG 1 Physiological effects of deletion and overexpression of the *mraZ* gene. (A) The *dcw* cluster of *E. coli*, showing the location of the P_{mra} promoter upstream of *mraZ* and highlighting the position of *mraZ* and *mraW* at the beginning of the cluster. (B) Spot dilution assay of WT and *mraZ* and *mraW* overexpressing MG1655 cells on LB plates containing 0.1 μg/ml trimethoprim. Shown from left to right are undiluted and 10^{-1} to 10^{-5} diluted samples of a mid-logarithmic-phase culture grown in LB with no antibiotic. (C) Spot dilution assay of WT and *mraZ* and *mraW* mutant MG1655 on LB plates containing 1 mM IPTG to fully induce gene expression. Shown from left to right are undiluted and 10^{-1} to 10^{-5} diluted samples of a mid-logarithmic-phase culture grown in LB with no induction. (D) Growth curves of the same strains as in panel B either uninduced or induced with 1 mM IPTG. V, vector.

110-amino-acid domain of unknown function that is novel among MTs but conserved in all MraW orthologs, including those in eukaryotes (see Table S3 in the supplemental material). Crystal structures of MraW from both *Thermotoga maritima* (19) and *E. coli* (23) are available, where MraW has been shown to form dimers in solution.

Transcription within the *dcw* cluster is complex, with as many as 12 different transcripts having been described (Ecogene database; www.ecogene.org), and reviewed in references 24 and 25. This transcript complexity may be necessary for proper regulation of the cell cycle in response to growth rate changes (26). The stationary-phase sigma factor RpoS and the LuxR family protein SdiA regulate the expression of the last genes in the *dcw* cluster, *ftsQA* and possibly *ftsZ* (27). SOS boxes precede the *ftsI* gene, and a gearbox promoter is located upstream of *ftsQ* (25). RNase E cleaves the polycistronic *ftsA-ftsZ* transcripts, affecting the decay of the *ftsA* and *ftsZ* mRNAs (28). Overall, the stability of the steady-state mRNAs from the *dcw* cluster varies (29).

Previous studies in other laboratories identified a σ^{70} promoter, P_{mra}, located upstream of *mraZ*, the first gene in the *dcw* cluster. P_{mra} drives the transcription of a polycistronic mRNA (11, 30, 31) extending through the first nine genes of the *dcw* cluster, including *ftsW* (11, 25) and possibly also through *murC*, but not reaching the essential *ftsQAZ* genes at the distal end of the cluster (32). Thus, the P_{mra} promoter is unlikely to be one of the upstream promoters driving the expression of the *ftsZ* gene (33). A putative σ^{70} promoter (11, 25) and a transcriptional start site located 38 bp upstream of the *mraZ* start site (25) have been identified previously. Intriguingly, there is an unusually long stretch of DNA between *mraZ* and its upstream gene, *cra* (*fruR*), with no apparent coding capacity (11). This, along with the importance of the 5′ *dcw* genes for cell division and PG synthesis, suggests that the P_{mra} promoter might be subject to regulation under some growth conditions. In this respect, recent microarray, promoter enrichment, and DNA-binding data implicate the pyruvate dehydrogenase complex regulator PdhR as a possible transcriptional regulator of P_{mra}, although the effects are very subtle (34).

Because of the inferred importance of MraZ and MraW in selective aspects of cell division and PG synthesis gene expression, as well as their widespread conservation in diverse bacteria, we decided to investigate their functions. In the present study, we focused mainly on MraZ and asked whether it is a transcriptional regulator on the basis of its structural homology to AbrB and MazE. We indeed found new evidence of a role for MraZ as a transcriptional regulator. We report that approximately 2% of the genes in the genome are differentially regulated when comparing a stationary-phase-grown *mraZ* null mutant to the wild-type (WT) parent. In addition, ~23% of *E. coli* genes are regulated by MraZ upon its overproduction during the early logarithmic phase. We also provide evidence that MraZ autoregulates its own expression from the P_{mra} promoter and can potentially repress the first 11 genes in the *dcw* cluster. We identify the locations of specific MraZ binding sequences involved in P_{mra} repression and demonstrate the DNA-binding activity of purified MraZ in electrophoretic mobility shift assays (EMSAs). Finally, we characterize a second MraZ binding site upstream of *mioC*.

MATERIALS AND METHODS

Bacterial strains, plasmids, and growth conditions. The bacterial strains and plasmids used in this study are described in Table 1. *E. coli* strains were grown at the required temperatures on either LB or minimal M-63 medium supplemented with either 0.2% glucose or 0.4% glycerol (35). When

TABLE 1 Bacterial strains and plasmids used in this study

Strain or plasmid	Genotype or phenotype	Source or reference
E. coli strains		
CGSC 8019	F$^-$ Δ*mraZ52* Δ*lacL* Δ*fnr267 rph-1*	40
CGSC 8021	F$^-$ Δ*mraW54* Δ*lacL* Δ*fnr267 rph-1*	40
DH5α	F$^-$ ϕ80d*lacZ*ΔM15 Δ(*lacZYA-argF*)*U169 recA1 endA1 hsdR17* (r_K^- m_K^+) *supE44* λ$^-$ *thi-1 gyrA relA1*	76
DH5α *phe*	F$^-$ ϕ80d*lacZ*ΔM15 Δ(*lacZYA-argF*)*U169 recA1 endA1 hsdR17*(r_K^- m_K^+) *supE44* λ$^-$ *thi-1 gyrA relA1 phe*::Tn*10d*Cm	77
JE6478	MG1655/pJE6448 Ap^r	This study
JE6430	MG1655/pDSW208 Ap^r	This study
JE6513	MG1655/pJE6496 Ap^r	This study
JE6517	MG1655/pJE6500 Ap^r	This study
JE6583	MG1655/pJE6584 Cm^r	This study
JE6598	WM2909/pRK415 Tet^r	This study
JE6599	WM2909/pJE6595 Tet^r	This study
JE6627	MG1655 *lacU169*/pDSW208/pJE6618 Ap^r Tet^r	This study
JE6628	MG1655 *lacU169*/pJE6500/pJE6618 Ap^r Tet^r	This study
JE6647	MG1655 *lacU169*/pDSW208/pJE6621 Ap^r Tet^r	This study
JE6648	MG1655 *lacU169*/pJE6500/pJE6621 Ap^r Tet^r	This study
JE6661	MG1655/pJE6653 Ap^r	This study
JE6707	MG1655 *lacU169*/pDSW208/pJE6695 Ap^r Tet^r	This study
JE6708	MG1655 *lacU169*/pJE6500/pJE6695 Ap^r Tet^r	This study
JE6710	MG1655 *lacU169*/pDSW208/pJE6696 Ap^r Tet^r	This study
JE6711	MG1655 *lacU169*/pJE6500/pJE6696 Ap^r Tet^r	This study
JE6713	MG1655 *lacU169*/pDSW208/pJE6697 Ap^r Tet^r	This study
JE6714	MG1655 *lacU169*/pJE6500/pJE6697 Ap^r Tet^r	This study
JE7023	MG1655 Δ*mraZ52* MG1655 *leuO*::*tet* × P1(CGSC8019) Tet^s prototroph	This study
JE7025	MG1655 Δ*mraW54* MG1655 *leuO*::*tet* × P1(CGSC8021) Tet^s prototroph	This study
JE7031	MG1655 Δ*mraZ52*/pDSW208	This study
JE7032	MG1655 Δ*mraZ52*/pJE6500	This study
JE7035	MG1655 Δ*mraW54*/pDSW208	This study
JE7108	MG1655 *lacU169*/pJE6640/pJE6618 Ap^r Tet^r	This study
MG1655	Sequenced λ$^-$ and F$^-$ derivative of K-12	78
MG1655 *lacU169*	*lac* mutant derivative of MG1655	Laboratory strain
WM2724	W3110 with native *ftsZ* + P_{trc}-*ftsZ-gfp* at λ *att* site	79
WM2909	W3110Δ*ftsL*::*kan* with Ts plasmid pTSA29-*ftsL* Kan^r Ap^r	Laboratory strain
Plasmids		
pBAD33	pACYC184 vector with P_{BAD} promoter; Cm^r	80
pBlueScriptII (pBSII)	Ap^r, with T3 and T7 promoters	Stratagene
pDSW208	P_{trc} promoter vector; Ap^r	81
pJE6448	pDSW208 EcoRI-HindIII with *mraZ-gfp*; Ap^r	This study
pJE6496	pDSW208 EcoRI-HindIII with *mraW-flag*; Ap^r	This study
pJE6500	pDSW208 EcoRI-HindIII with *mraZ-gluglu*; Ap^r	This study
pJE6584	pBAD33 KpnI-HindIII with *mraZ-gluglu*; Cm^r	This study
pJE6595	pRK415 BamHI-KpnI with ~2,700-bp PCR fragment encompassing 563 bp upstream of *mraZ* to downstream *ftsL*	This study
pJE6617	pBSII SmaI with same ~2,700-bp PCR fragment as pJE6595 but with MraZR15A mutation	This study
pJE6618	WT *mraZ*::*lacZ* translational fusion vector; pUI523A::593-bp PCR fragment from *mraZ* (563 bp upstream and 30 bp within gene); Tet^r	This study
pJE6621	O_1 *mraZ*::*lacZ* translational fusion in pJE6618 with TGGGG-to-ATCGG mutation in DR2; Tet^r	This study
pJE6640	pDSW208 EcoRI-HindIII with *mraZR15A-gluglu*; Ap^r	This study
pJE6695	O_2 *mraZ*::*lacZ* fusion in pJE6618 with TGGGA-to-AGGCA mutation in DR1 and TGGGG to ATCGG mutation in DR2; Tet^r	This study
pJE6696	O_3 *mraZ*::*lacZ* fusion in pJE6618 with TGGGG-to-ATCGG mutation in DR2 and TGGGA to ATCGA mutation in DR3; Tet^r	This study
pJE6697	O_4 *mraZ*::*lacZ* fusion in pJE6618 with TGGGA-to-AGGCA mutation in DR1, TGGGG-to-ATCGG mutation in DR2, and TGGGA-to-ATCGA mutation in DR3; Tet^r	This study
pJE6653	pDSW208 EcoRI-HindIII with *mraZ-mraW*; Ap^r	This study
pJE6761	pDSW208 NcoI-HindIII with *his-mraZ-gluglu*; Ap^r	This study
pJE6762	pDSW208 NcoI-HindIII with *his-mraZR15A-gluglu*; Ap^r	This study
pJE7145	pBAD33 KpnI-HindIII with *mioC*	This study
pRK415	Low-copy-number IncP plasmid; Tet^r	82
pUI523A	Promoterless *lacZ* translational fusion vector; Tet^r	38

required, tetracycline (Tet) at 20 μg/ml, kanamycin (Kan) at 25 μg/ml, chloramphenicol (Cm) at 20 μg/ml, and ampicillin (Ap) at 150 μg/ml were added to the growth medium. Cultures were grown anaerobically in anaerobic chambers with BD BBL Plus anaerobic system envelopes and indicators, and LB and minimal M-63 plates were supplemented with 20 mM KNO_3 as the terminal electron acceptor.

DNA manipulations and analysis. For the primers used in this study, see Table S1 in the supplemental material. Standard protocols or the manufacturer's instructions were followed to isolate plasmid DNA, as well as for restriction endonuclease, DNA ligase, PCR, and other enzymatic treatments of plasmids and DNA fragments. To eliminate potential impurities, DNA fragments were drop dialyzed against autoclaved water for 1 h on 0.025-μm disc filters (Millipore, Billerica, MA) prior to ligation reactions. Enzymes were purchased from New England BioLabs, Inc. (Beverly, MA); Promega Corp. (Madison, WI); and Invitrogen (Carlsbad, CA). Plasmids and DNA fragments were purified with the Wizard SV miniprep and PCR Cleanup kits from Promega (Madison, WI). Phusion DNA polymerase was used as the high-fidelity PCR enzyme (New England BioLabs). The final versions of all relevant clones were verified by sequencing. Modified and unmodified oligonucleotides were purchased from Sigma-Aldrich.

Transcriptome sequencing (RNA-seq) experiments. Whole-genome transcriptome analyses were performed at two different stages of the cell cycle. Gene expression was assayed in an *mraZ* null mutant (JE7031) grown to a high cell density (optical density at 600 nm [OD_{600}] of ≥1.4) and compared to that in the WT (JE6430). Ten-milliliter volumes of the respective cultures were spun, treated with RNAlater (Life Technologies, Grand Island, NY) by following the manufacturer's instructions, frozen, and stored at −70°C prior to RNA extraction. In addition, gene expression was also assayed in MraZ-overproducing cells (JE6517) and compared to that in WT cells containing the empty vector (JE6430); both were grown to early log phase (OD_{600} of ≤0.1). Two-hundred-milliliter volumes of the respective cultures were processed in a manner similar to that described above. All cultures were grown in triplicate and processed independently.

RNA extraction. RNA was extracted with Invitrogen TRIzol Reagent (catalog no. 15596018), followed by genomic DNA removal and cleaning with the Qiagen RNase-Free DNase Set kit (catalog no. 79254) and the Qiagen Mini RNeasy kit (catalog no. 74104). An Agilent 2100 Bioanalyzer was used to assess the integrity of the RNA samples. Only RNA samples with integrity numbers between 8 and 10 were used.

RNA sequencing. The Applied Biosystems SOLiD Total RNA-Seq kit (catalog no. 4445374) was used to generate the cDNA template library. The SOLiD EZ Bead system was used to perform emulsion clonal bead amplification to generate bead templates for SOLiD platform sequencing. Samples were sequenced on the 5500XL SOLiD platform. The 50-base short-read sequences produced by the 5500XL SOLiD sequencer were mapped in color space with SOLiD LifeScope software version 2.5 by using the default parameters against the genome of *E. coli* K-12 strain MG1655 (WIS_MG1655_m56) reference genome, and both the FASTA and GFF files were obtained from the *E. coli* Genome Project at the University of Wisconsin—Madison (http://www.genome.wisc.edu/sequencing.htm). The output of the whole-transcriptome analysis generated a gene count file with the base counts summed to a single value across the entire gene length and with the number of reads per kilobase of transcript per million mapped reads (RPKM) also given for each gene, a BAM file containing the sequence of every mapped read and its mapped location, one pair of *.wig files giving the mapped counts at each base position, and a statistical summary on alignment and filtering report.

Transcriptome and pathway enrichment analyses. RNA-seq data were filtered to remove genes in the high- or low-OD sample sets with fewer than two replicates with nonzero counts per million for each condition. The bioconductor package edgeR (36) was used to identify the degree of statistical differential expression between the WT and the *mraZ* mutant, as well as WT and *mraZ* overexpression conditions, for each gene. Separate analyses of data from high- and low-OD_{600} conditions were conducted. Genes were ranked according to the resulting *P* values, and these rankings were used as input to Gene Set Enrichment Analysis (GSEA) software (37). This algorithm identifies gene sets whose members are statistically significantly enriched among genes at the top (or bottom) of a list of ranked genes. We used the "GSEA preranked" setting so that we could enter our ranked list as direct input, thus bypassing the ranking step set by GSEA. As input, GSEA takes user-defined gene sets grouped according to areas of potential interest. For gene sets, we used the files "func-associations.col" and "pathways.col" in the set of *E. coli*-specific files from the EcoCyc web resource (ecocyc.org). Gene sets were included only if the number of genes in the set present in the expression data was at least 10.

Microscopy. Cells expressing green fluorescent protein (GFP) or mCherry fusions were grown in LB plus antibiotics and embedded in 1% LB-agarose on a microscope slide. To image these cells, we used an Olympus BX60 fluorescence microscope equipped with a 100× numerical aperture 1.4 objective and GFP, 4′,6-diamidino-2-phenylindole (DAPI), and tetramethyl rhodamine isocyanate (for mCherry) filter sets. Grayscale images from each channel were captured with a Hamamatsu ORCA II charge-coupled device camera and HCImage software and imported into Adobe Photoshop for pseudocoloring and image layering.

Construction of translational *lacZ* fusions and β-galactosidase assays. Plasmid pJE6618 harbors the WT *mraZ-lacZ* translational fusion, which contains a 593-bp PCR fragment from the *mraZ* gene (563 bp upstream and 30 bp within the gene) fused to *lacZ* in pUI523A (38). Combinatorial PCR, as described previously (39), was used to mutate the three direct repeats (DRs) in the *mraZ* operator to construct fusions O_1, O_2, O_3, and O_4 in plasmids pJE6621, pJE6695, pJE6696, and pJE6697, respectively (Table 1).

β-Galactosidase assays were performed as described elsewhere (38). The data provided are the averages of at least two separate experiments each performed in duplicate. Standard deviations were always ≤15%. Protein concentrations of cell extracts were determined with the bicinchoninic acid (BCA) protein assay kit (Thermo Scientific, Waltham, MA) with bovine serum albumin as the standard.

P1 transductions. Standard protocols were used to mobilize genetic markers from existing strains by phage P1*vir* transductions (35). All of the strains used are listed in Table 1. JE7023 (MG1655 *mraZ*) and JE7025 (MG1655 *mraW*) were constructed by P1 transduction with CGSC8019 and CGSC8021 (40), respectively, as donors and MG1655 *leuO*::Tn*10* as the recipient. After selecting for prototrophy and scoring for Tet^s, the resulting *mraZ* and *mraW* deletion mutant genes were PCR amplified from the chromosome of the transductants and verified by sequencing.

DNA labeling. The *mraZ* and *mioC* regulatory regions were PCR amplified with biotinylated primers. A 240-bp *mraZ* biotinylated fragment was amplified with primers 1922 and 1923, whereas *mioC* was amplified with primers 2045 and 2046 to form a 238-bp fragment. Competitor DNA fragments were also PCR amplified with nonbiotinylated primers with the exact same DNA sequences. The DNA amplification efficiencies were similar when using labeled and unlabeled primers. DNA concentrations were calculated after reading the OD_{260}s of several dilutions of the purified fragments with a UV-1601 UV-visible spectrophotometer (Shimadzu, Kyoto, Japan).

MraZ binding and competition assays. The final reactant concentrations in the 25-μl DNA-binding reaction mixtures were 1× binding buffer, 5 mM $MgCl_2$, 0.04% Nonidet P-40 (NP-40), 2 mM spermidine trihydrochloride, ~0.35 pmol of a biotin-labeled double-stranded 240-bp *mraZ* or 238-bp *mioC* fragment, 40 ng/ml LightShift poly(dI · dC) nonspecific competitor DNA (Thermo Scientific, Waltham, MA), water, and purified MraZ in storage or dilution buffer at the appropriate concentrations (see recipes below). The presence of spermidine in the binding reaction mixtures increases the binding specificity for other transcriptional regulators (41). The MraZ dilutions were done in 1× dilution buffer. After the addition of MraZ, the reaction mixtures were incubated at room temperature for 20 min, and immediately 4 μl (~1/6) of each reaction mixture was loaded into the prerun gels described in the next section. For

each experiment, both gels in the electrophoresis tank contained identical samples and therefore were run in duplicate. For competition experiments, the specific competitor DNA at the appropriate concentration was added after MraZ addition, prior to incubation. The 10× MraZ binding buffer contained 200 mM Tris (pH 7.5), 50 mM KCl, 5 mM $MgCl_2$, and 1 mM dithiothreitol (DTT). The 1× MraZ dilution buffer contained 25 mM Tris (pH 7.5), 150 mM KCl, 5 mM $MgCl_2$, and 0.5 mM DTT. The 10× gel loading buffer contained 250 mM Tris (pH 7.5), 0.2% bromophenol blue, and 40% glycerol.

Electrophoretic mobility shift assays (EMSAs). Electrophoresis was performed in Mini Protean 3 cells (Bio-Rad, Hercules, CA) with 5% gels made with a 40% stock of 29:1 acrylamide-bisacrylamide and 0.5× Tris-borate-EDTA (TBE). Gels were run at 4°C for approximately 20 min at 85 V and for an additional 1 h at 60 V. Both the gels and the running buffer contained a final concentration of 200 μM spermidine. After electrophoresis, the DNA fragments were wet transferred in 0.5× TBE to Biodyne B nylon membranes (Thermo Scientific, Waltham, MA) for 30 min at 385 mA and UV-cross-linked with a UV Stratalinker 1800 (Agilent Technologies, Santa Clara, CA) by using the auto-cross-link setting. The Chemiluminescent Nucleic Acid Detection Module (Thermo Scientific, Waltham, MA) was used for detection in accordance with the manufacturer's instructions. The blots were exposed on Hyblot CL film (Denville Scientific Inc., South Plainfield, NJ).

Protein purifications. His_6-MraZ-GluGlu and His_6-MraZR15A-GluGlu were purified from 8 liters of MG1655 containing plasmid pJE6761 or pJE6762 (Table 1) encoding full-length WT or R15A mutant MraZ, respectively. These plasmids are derivatives of pDSW208, which contains an isopropyl-β-D-thiogalactopyranoside (IPTG)-inducible P_{trc} promoter. Cells were grown at 30°C for approximately 3 h to an OD_{600} of ~0.6, induced with 1 mM IPTG for ~90 min, and collected by centrifugation. Pellets were washed once in MraZ lysis buffer (25 mM Tris [pH 7.5], 200 mM NaCl, 5 mM $MgCl_2$) and stored at −70°C. Phenylmethylsulfonyl fluoride was used at a 1 mM final concentration. Cells were lysed by three passages through a French pressure cell (SLM Aminco, Rochester, NY). The cell lysates were clarified by centrifugation at 11,000 × *g* for 20 min at 4°C and incubated on ice for 30 min in the presence of 2 mg/ml lysozyme and DNase. TALON metal affinity resin (Clontech, Mountain View, CA) was used for purifications by following manufacturer's instructions. Crude extracts were incubated with the resin for 2 h at 4°C prior to column purification in the presence of 5 mM imidazole. After washes in MraZ lysis buffer containing 5, 20, and 30 mM imidazole and elution in MraZ lysis buffer with 500 mM imidazole, the proteins were dialyzed twice at 4°C for ~18 h against buffer I (25 mM Tris [pH 7.5], 150 mM KCl, 5 mM $MgCl_2$, 1 mM DTT, 20% glycerol, 100 mM NaCl) and then buffer II (same as buffer I but with no NaCl). The purified proteins were resuspended in 100-μl aliquots and quick frozen in a dry-ice–ethanol bath prior to storage at −80°C. The BCA assay (Thermo Scientific, Rockford, IL) was used to determine protein concentration. The purification procedure yielded proteins that were ≥95% pure (data not shown).

Immunoblot analysis. Crude extracts and purified protein were resuspended in SDS loading buffer, boiled for 10 min, and separated by SDS-PAGE in Mini Protean 3 cells (Bio-Rad, Hercules, CA) with 12 or 18% gels made with a 40% stock of 29:1 acrylamide-bisacrylamide. Proteins were transferred to nitrocellulose membranes with a wet apparatus. In addition to the N-terminal His_6 tag, a C-terminal GluGlu epitope (EE EVMPME) (42) was used to tag MraZ for Western blot analysis. The sequence encoding the GluGlu tag was added by using combinatorial PCR as described previously (39). The DNA fragments were amplified from an *mraZ*-containing PCR product obtained by colony PCR. Plasmid pJE6500 contains carboxy-terminally GluGlu-tagged full-length *mraZ*. The primary antibodies used for immunoblotting were monoclonal anti-His_6 (Sigma-Aldrich, St. Louis, MO) or monoclonal anti-GluGlu (Covance Research Products, Inc., Emeryville, CA) antibodies at 1:5,000. Anti-mouse secondary antibodies conjugated to horseradish peroxidase (HRP) were used at 1:10,000. SuperSignal West Pico Chemiluminescent Substrate (Thermo Scientific) was used as the substrate for HRP detection.

Other reagents. *o*-Nitrophenyl-β-D-galactopyranoside, spermidine trihydrochloride (minimum 98%), and antibiotics were purchased from Sigma Chemical Co., St. Louis, MO. NP-40 was purchased from Thermo Scientific, Waltham, MA. GeneMate LE agarose was purchased from Bio-Express, Kaysville, UT. All of the other chemicals used in this work were reagent grade.

RESULTS

Phenotypic analysis of cells after loss of MraZ or MraW. The *dcw* cluster (Fig. 1A) and its first two genes, *mraZ* and *mraW*, are highly conserved in prokaryotes (9, 10). Using the web server hmmer.janelia.org, we identified orthologs of MraZ in 2,184 out of 2,259 significant query matches within bacterial species (see Table S2 in the supplemental material) and orthologs of MraW in 4,184 out of 4,402 (see Table S3). Interestingly, MraW was also found in 161 eukaryote species (see Table S3), consistent with a previous report of MraW homologs in eukaryotes (6). Thus, *mraZ* and *mraW* are very highly conserved and MraW is more universal.

Despite their conservation and prevalence, nonpolar deletions of *mraZ* and *mraW* have no detectable phenotypes under standard laboratory conditions in *E. coli* (40, 43, 44) and *B. subtilis* (45). We confirmed that unmarked deletion mutations in both genes (40) in the MG1655 strain background are indeed nonessential for viability and subsequently searched for conditional phenotypes associated with the removal of these genes. The growth rates of cells lacking *mraZ* or *mraW* were indistinguishable from those of the WT parent during aerobic growth in LB at 37°C, anaerobic growth on LB with nitrate as the terminal electron acceptor, or both aerobic and anaerobic growth on M-63 minimal medium supplemented with glycerol as the sole carbon source (data not shown). Additionally, viability after a 12-day extended period in stationary phase was not affected in the *mraZ* and *mraW* mutants compared to the WT parent strain, although general viability was down by 2 logs (data not shown).

We then searched for differences in antibiotic susceptibility. We found that the MICs for both mutants and the WT parent strain were the same in the presence of Ap; the β-lactam amoxiclav; the cephalosporin cephapirin; cefoxitin, which interferes with cell wall synthesis; colistin, which alters both inner and outer membrane integrity; and the DNA gyrase inhibitor nalidixic acid. Notably, however, we did find that the *mraZ* mutant was more resistant to the dihydrofolate reductase (DHFR) inhibitor trimethoprim than the WT parent (Fig. 1B). In contrast, the *mraW* mutant was more sensitive to trimethoprim than was the WT strain, consistent with data from the Porteco website (Porteco.org).

MraZ overproduction is lethal and perturbs cell division. The difficulty in uncovering a growth phenotype for the *mraZ* or *mraW* null mutant prompted us to investigate the effect of *mraZ* or *mraW* overexpression. Although overproduction of MraW by IPTG induction of plasmid pDSW208-P_{trc}-*mraW* (called pDSW208-*mraW* here) had no phenotype in rich (LB) growth medium, overproduction of pDSW208-P_{trc}-*mraZ* (called pDSW208-*mraZ* here) with IPTG induction was lethal (Fig. 1C). IPTG concentrations of ≥50 μM prevented colony formation (data not shown). Cessation of growth after the overexpression of *mraZ* was also observed in growth curves (Fig. 1D). Notably, MraZ-overproducing cells filamented (see Fig. S1 in the supplemental material), suggesting that cell division is affected and may be a signifi-

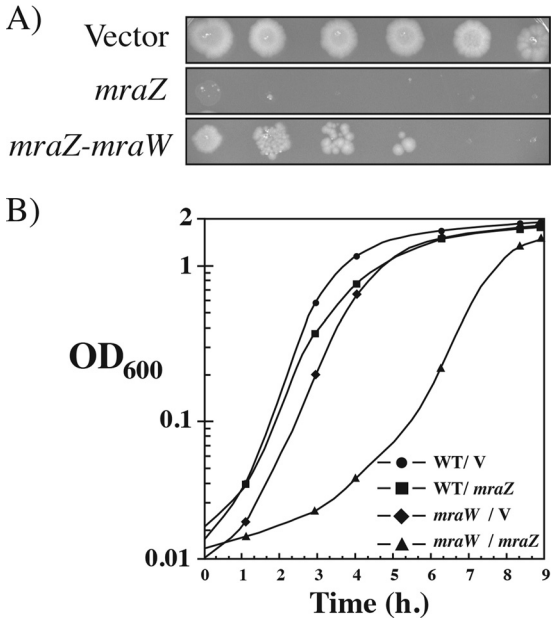

FIG 2 Antagonistic effect of MraW on MraZ. (A) Spot dilution assay of WT MG1655 containing the pDSW208 vector alone, pDSW208-*mraZ*, or pDSW208-*mraZ-mraW* on LB plates containing 1 mM IPTG to fully induce gene expression. Shown from left to right are undiluted and 10^{-1} to 10^{-5} diluted samples of a mid-logarithmic-phase culture grown in LB with no induction. (B) Growth curves of WT MG1655 and the *mraW* null mutant in LB without IPTG containing either the pDSW208 vector alone (V) or pDSW208-*mraZ*.

cant cause of the lethality seen. Cells containing the pDSW208-*mraZ* plasmid in minimal medium supplemented with glycerol as the sole carbon source filamented and formed bulges (data not shown) even without IPTG induction, suggesting that excess MraZ is more toxic when cells are grown in minimal medium than when grown in LB (see Fig. S2).

Our results suggest that cell filamentation and killing are directly correlated with increased cellular levels of MraZ. Consistent with this, when expressed from the more tightly repressed arabinose-inducible promoter in pBAD33, filamentation increased as MraZ was overproduced by induction with arabinose, but there was no killing (data not shown). These phenotypes were not caused by induction of the SOS response, as *recA* mutant cells exhibited similar phenotypes (data not shown).

MraW suppresses the toxic effects of MraZ overproduction. The *mraZ* and *mraW* genes are nearly always adjacent, and in *E. coli* they are separated by 1 nucleotide (nt). It has been suggested that conservation of a gene pair indicates that the proteins in the pair interact (46). To test this notion, we co-overexpressed *mraW* and *mraZ*, either in *cis* in their native *mraZ-mraW* gene context or in *trans* on separate plasmids. In both cases, MraZ toxicity was significantly reduced (Fig. 2A), suggesting that MraW antagonizes MraZ overproduction toxicity (see also below). Consistent with this antagonistic effect, we found that uninduced pDSW208-*mraZ*, normally not toxic in a WT background, inhibited the growth of an *mraW* null mutant (Fig. 2B). Thus, in addition to an increased sensitivity to trimethoprim (Fig. 1B), this is a new phenotype of an *mraW* null mutant and suggests that MraW may regulate MraZ activity.

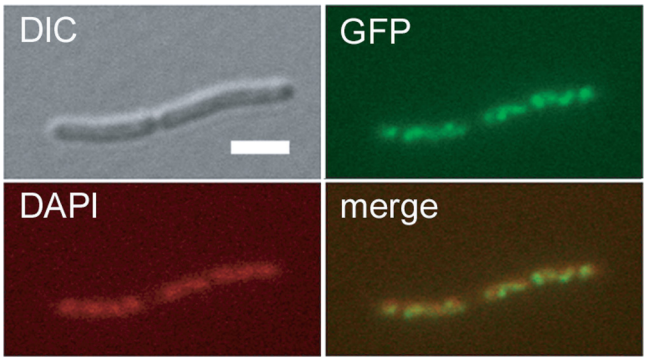

FIG 3 MraZ localizes to the nucleoid. WT MG1655 containing an *mraZ-gfp* fusion in pDSW208 was grown in LB to an OD_{600} of ~0.2 with no IPTG induction. Cells were moderately inhibited for septation even under these uninduced conditions because of leaky expression from the plasmid *trc* promoter. Differential interference contrast (DIC), DAPI-stained, MraZ-GFP fluorescence, and merged DAPI-GFP images of a representative dividing filament are shown (scale bar, 3 μm).

MraZ overproduction destabilizes the divisome but does not affect FtsZ levels or prevent Z ring assembly. The filamentation of MraZ-overproducing cells prompted us to ask whether the levels or localization of the key divisome component FtsZ were perturbed. To enable us to measure MraZ levels while also monitoring FtsZ levels, we fused the GluGlu epitope tag to the 3′ end of *mraZ* (Table 1 and Materials and Methods). This fusion conferred the same overproduction phenotype as untagged MraZ. We found that MraZ overproduction did not affect cellular FtsZ levels and allowed normal localization of an FtsZ-GFP fusion to Z rings (data not shown). Moreover, an increased copy number of the last three *dcw* genes, *ftsQAZ* (Fig. 1A), which can alleviate many cell division defects, did not suppress the killing phenotype (data not shown). On the other hand, higher but normally nonlethal levels of MraZ became lethal at the permissive temperature (30°C) in an *ftsZ*84 mutant, which has lower GTPase activity and subunit turnover at the permissive temperature (47, 48) (data not shown). A similar synthetic lethal phenotype with normally nonlethal levels of MraZ was observed in Δ*minCDE* mutant cells, which assemble extra Z rings at inappropriate locations throughout the cell (49). These results support the ideas that MraZ overproduction perturbs the level or activity of a divisome component(s) and that this perturbation, combined with partially defective FtsZ or MinCDE, causes divisome collapse.

MraZ localizes to the nucleoid. Because of the similarity between the N-terminal domain of MraZ and the N-terminal DNA-binding domains of AbrB and MazE, we decided to investigate whether MraZ binds DNA, perhaps acting as a transcriptional regulator of *dcw* genes. As a first step to test this idea, we constructed carboxy-terminal GFP and mCherry fusions to both MraZ and MraW to investigate their cellular localization. The MraZ fusions were toxic when overproduced, suggesting that they retained at least partial function. Cells containing an uninduced MraZ-GFP fusion on pDSW208 exhibited fluorescence throughout the nucleoid, with several areas of brighter intensities (Fig. 3). Cytoplasmic fluorescence was undetectable above the background, indicating that MraZ strongly bound DNA. Uninduced levels of MraZ-mCherry displayed a similar nucleoid localization pattern (data not shown). Higher induced levels of MraZ-GFP

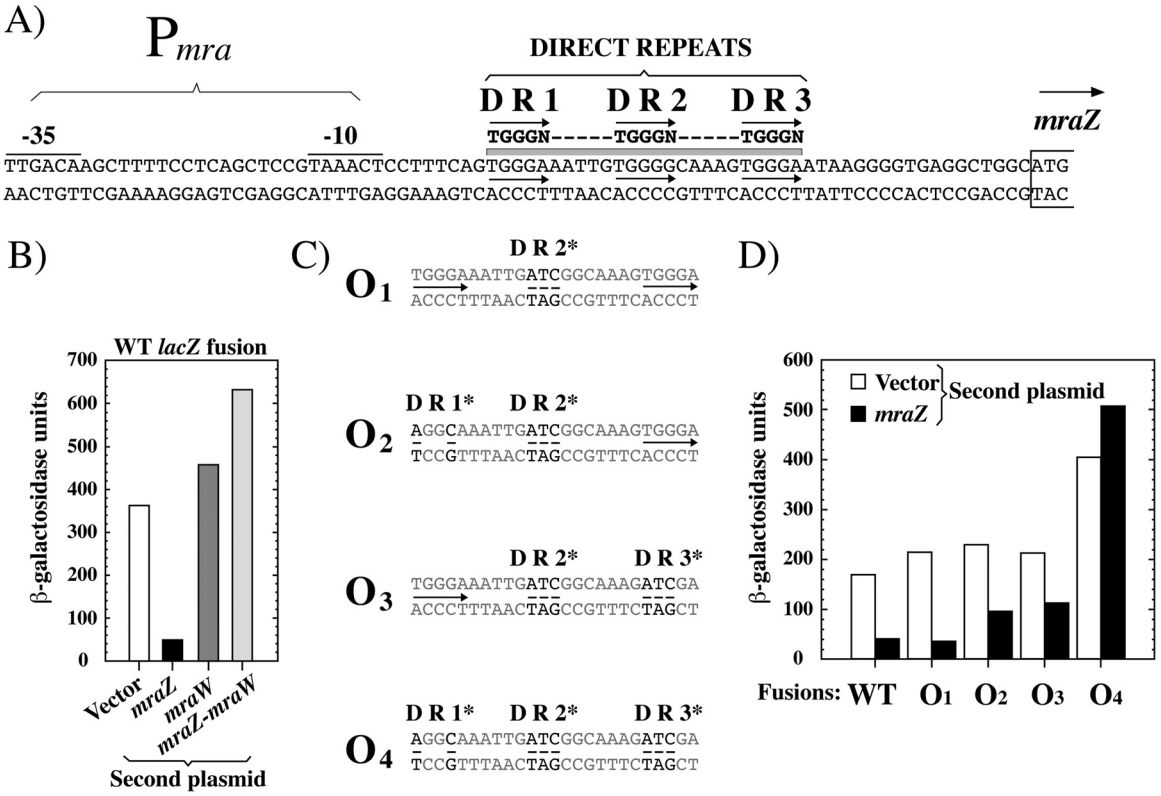

FIG 4 Negative autoregulation by MraZ. (A) The DNA sequence of the *mraZ* regulatory region is shown, highlighting P_{mra} and the O_{WT} sequence, TGGGN-N_5-TGGGN-N_5-TGGGN. DR1, DR2, and DR3 represent the three DRs separated by the 5-nt spacer regions. (B) β-Galactosidase assays with the WT *mraZ-lacZ* fusion. WT MG1655 cells carrying a pDSW208 plasmid with no insert (vector) or expressing *mraZ*, *mraW*, or both *mraZ* and *mraW* were assayed for expression of the *mraZ-lacZ* reporter on a compatible plasmid (pJE6618). β-Galactosidase activity is expressed in μmol/min/mg protein. Standard deviations were ≤15%. (C) Four different mutant P_{mra} operator sites are shown. Asterisks indicate the mutagenized DRs. The mutations in the DRs are underlined. (D) Comparison of the β-galactosidase activities of the WT *mraZ-lacZ* reporter or mutant *mraZ-lacZ* (O_1 to O_4) reporters regulated by expression from pDSW208 (vector) or (pDSW208/*mraZ*). Cells were induced with 50 μM IPTG for 30 min. β-Galactosidase activity is expressed in μmol/min/mg protein. One representative experiment is shown.

also localized throughout the nucleoid, still with no detectable nonnucleoid localization. In contrast, the MraW-GFP and MraW-mCherry fusions localized uniformly in the cytoplasm (data not shown). These results agree with previous general localization studies reported earlier for *E. coli* proteins (Genobase; http://ecoli.naist.jp/GB6/search.jsp). This localization of MraZ throughout most of the nucleoid but with a nonuniform pattern at low levels of induction is consistent with MraZ binding to different sites on the chromosomal DNA, and it supports the hypothesis that MraZ might have several chromosomal targets, which we set out to test further.

MraZ negatively regulates its own expression from P_{mra}. As both AbrB and MazE negatively regulate their own expression (50, 51), we decided to test whether MraZ does the same by repressing transcription from P_{mra}. To define the potential boundaries of the P_{mra} promoter, we constructed pJE6595, a low-copy-number plasmid that contains a 2.7-kb fragment including the unusually long 563-bp regulatory region upstream of *mraZ* and extending through *mraZ-mraW-ftsL* (Table 1). This plasmid was able to complement the FtsL depletion strain WM2909 (see Fig. S3 in the supplemental material), suggesting that it contains the key elements for regulation of P_{mra} expression. The basic promoter structure of P_{mra} is shown in Fig. 4A, including the −35 and −10 sequences typical of σ^{70}-dependent promoters (52).

To measure transcription from P_{mra} and potential regulation by MraZ, we fused the 563-bp regulatory region upstream of *mraZ* plus 10 codons of the *mraZ* coding region to *lacZ* to make an *mraZ-lacZ* reporter. We then measured β-galactosidase production in response to excess MraZ produced from a compatible plasmid, pDSW208-*mraZ*, induced with a low, nonlethal level of IPTG (Fig. 4B). We found that increased expression of *mraZ* reduced the expression of the *mraZ-lacZ* fusion by ~7-fold, compared to the vector alone (compare white with black bars). In contrast, the increased expression of *mraW* from pDSW208-*mraW* had little effect on *mraZ-lacZ* expression (Fig. 4B), consistent with its lack of toxicity in LB. When *mraW* was present downstream of *mraZ* in its normal context in pDSW208-*mraZ-mraW*, β-galactosidase values were nearly 2-fold higher than those obtained with the vector alone and nearly 10-fold higher than those obtained with pDSW208-*mraZ* at the same level of IPTG (compare light gray with black bars). These results strongly suggest that MraZ represses its own promoter, P_{mra}, and that the MraW negative modulatory effect on MraZ described above leads to derepression of P_{mra} expression, possibly by preventing DNA binding by MraZ.

Examination of the *mraZ* regulatory region revealed the motif TGGGN-5 nt-TGGGN-5 nt-TGGGN, containing three successive TGGGN DRs separated by two consecutive 5-nt spacers. Interest-

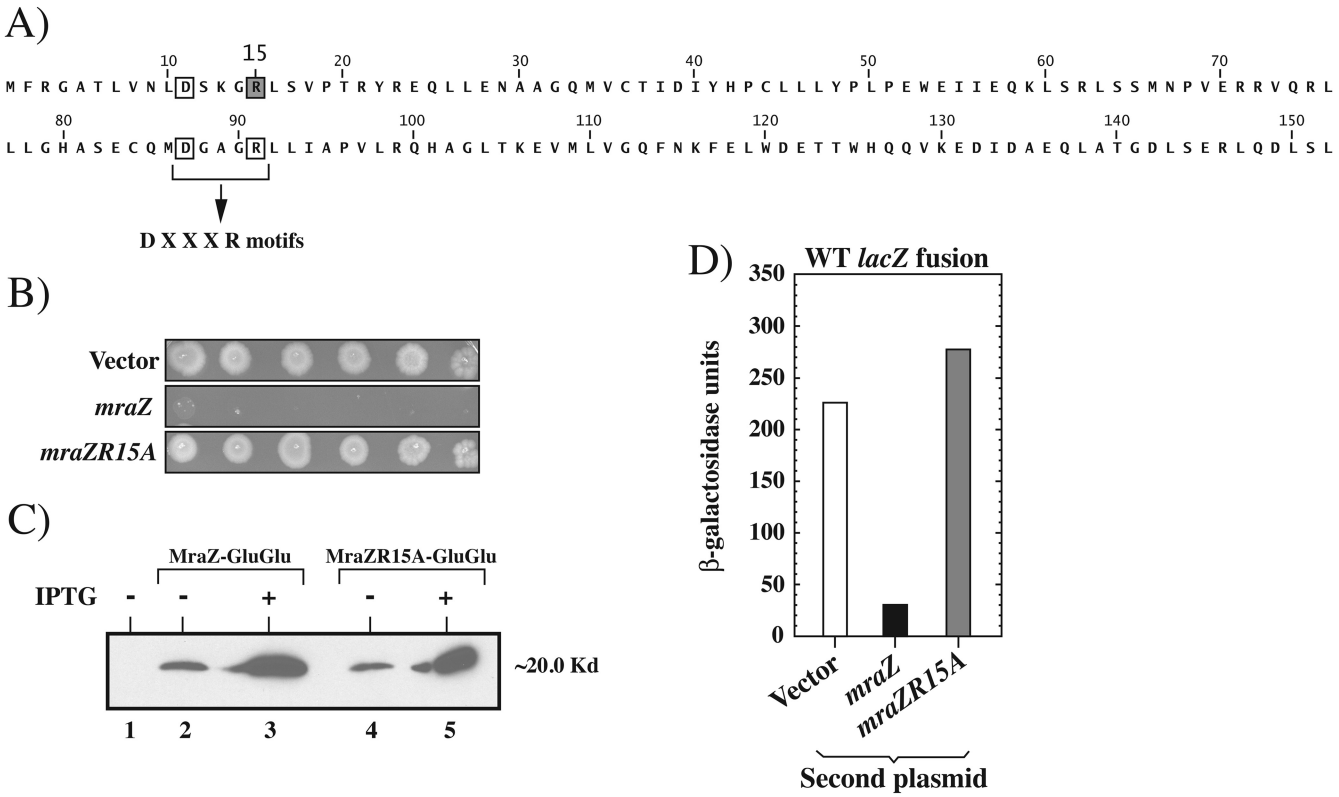

FIG 5 Characterization of the MraZR15A DNA-binding mutant. (A) Sequence of the MraZ protein from *E. coli*, representing the two copies of the UPF0040 fold (19), including amino acids 1 to 76 (top row) and 77 to 152 (bottom row). The two DXXXR motifs are highlighted; they correspond to amino acids D11 to R15 and D87 to R91. Arginine R15 (shaded square) in the first motif was mutated to alanine in the MraZR15A mutant. (B) Spot dilution assay of WT MG1655 containing the pDSW208 vector, pDSW208-*mraZ*, or pDSW208-*mraZR15A* on LB plates containing 1 mM IPTG to fully induce gene expression. (C) Levels of MraZR15A are similar to those of MraZ. WT MG1655 cells containing the pDSW208 vector (lane 1), pDSW208-*mraZ-gluglu* (lanes 2 and 3), or pDSW208-*mraZR15A-gluglu* (lanes 4 and 5) were grown in LB to an OD_{600} of ~0.2. Cells expressing *mraZ* on the plasmid were either left uninduced (lanes 2 and 4) or induced (lanes 3 and 5) with 1 mM IPTG and grown for an additional 2 h. Aliquots were normalized for total protein and subjected to SDS-PAGE. Blots were detected with anti-GluGlu antibodies. The location of 20 Kd is where the 20-kDa molecular size marker runs. (D) β-Galactosidase assays comparing the effects of pDSW208 (vector), (pDSW208/*mraZ*), and (pDSW208/*mraZR15A*) on the *mraZ-lacZ* reporter after induction with 50 μM IPTG for 30 min. β-Galactosidase activity is expressed in μmol/min/mg protein. One representative experiment is shown.

ingly, this repeat resembles the TGGNA motif involved in DNA recognition by AbrB in *B. subtilis* (53). As this repeat region is located 8 nt downstream from the P_{mra} promoter (Fig. 4A), it is consistent with the idea that these DRs constitute an operator site for MraZ binding.

To test this hypothesis, we constructed additional *mraZ-lacZ* fusions containing mutations in the TGGGN DRs singly or in combination. We called the WT sequence operator O_{WT} and the mutant sequences O_1 to O_4 (Fig. 4C). The expression results are shown in Fig. 4D; in general, the mutant *mraZ-lacZ* fusions were derepressed, even when *mraZ* was overexpressed, compared to the WT fusion. Interestingly, the effect of mutation of the DRs is additive; the *lacZ* fusion to the O_1 operator, in which the middle DR (DR2) is mutated, was still repressed, but the *lacZ* fusion to the O_4 mutant operator, in which all of the DRs are mutated, was totally derepressed, irrespective of whether MraZ was overproduced or not. Thus, MraZ represses the expression of P_{mra} and the *mraZ* gene and the DRs constitute DNA elements necessary for this repression. As we cannot rule out the possibility that promoter function and/or a transcription start site(s) may have been perturbed as a consequence of the mutagenesis, we next tested DNA binding with purified MraZ (see below).

A point mutation in the putative DNA-binding domain of MraZ eliminates its toxicity. If MraZ is a transcriptional regulator, then the killing phenotype observed upon its overproduction is most likely caused by inappropriate regulation of gene expression at the O_{WT} operator located upstream of *mraZ* and/or at additional genomic targets. Thus, overproduction of a mutant MraZ protein unable to bind to DNA should not be toxic. Arginine 15 (R15) in MraZ is conserved in AbrB from *B. subtilis* (14, 15) and MazE from *E. coli* (16). An R16A mutation at the equivalent location in MazE abolishes DNA binding (16, 51). R15 of MraZ forms part of the first DXXXR DNA-binding motif of MraZ present in the two tandem homologous copies of the UPF0040 fold (Fig. 5A) (6, 18). We therefore decided to mutate this arginine, predicting that it would abolish MraZ binding to DNA.

We found that MraZR15A is not toxic to cells, even when overproduced by full IPTG induction, in contrast to the WT protein (Fig. 5B). The stability of the MraZR15A mutant protein is similar to that of WT MraZ under uninduced and induced conditions (Fig. 5C), suggesting that the mutation inactivates a specific function of MraZ. We calculate that there was an ~10-fold increase in protein concentration in induced versus uninduced cells, with the caveat that MraZ was lethal to cells at this concentration of IPTG.

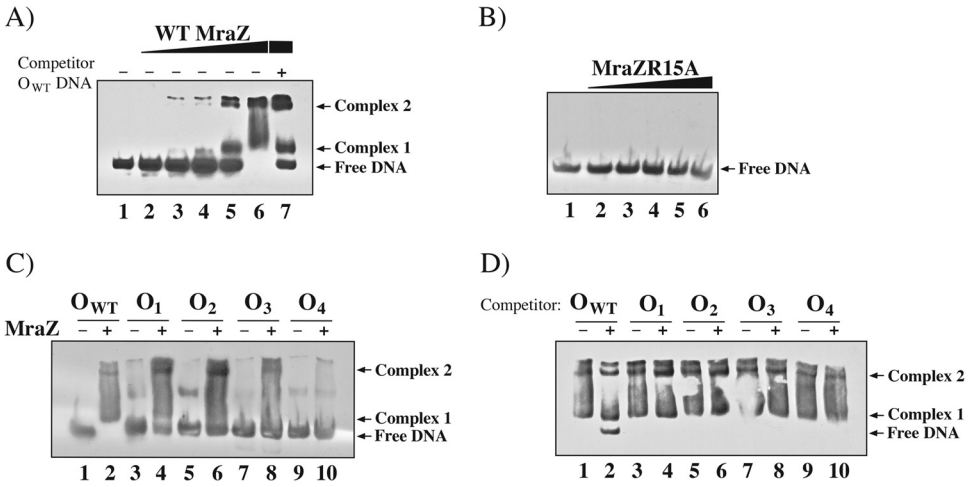

FIG 6 Binding of MraZ to the *mraZ* regulatory region. (A) Binding of increasing concentrations of WT MraZ to biotinylated O_{WT} in EMSAs. About 0.3 pmol of a biotinylated 240-bp fragment containing the *mraZ* regulatory region was incubated with 3.2 (lane 2), 6.4 (lane 3), 10.7 (lane 4), 32 (lane 5), or 96 (lane 6) pmol of MraZ protein. The components in lane 7 were similar to those in lane 6, with the addition of an approximately 8× molar excess of unlabeled *mraZ* DNA. Lane 1 is biotinylated *mraZ* DNA alone. Complexes 1 and 2 are the two specific complexes observed. (B) Binding of increasing concentrations of mutant MraZR15A to biotinylated O_{WT}. The protein concentrations were similar to those in panel A. Lane 1 is biotinylated *mraZ* DNA alone. (C) Binding of MraZ to WT (O_{WT}) and mutant (O_1 to O_4) operators. About 0.3 pmol of a labeled double-stranded 240-bp fragment containing O_{WT} was incubated with ~0.09 nmol of MraZ protein, equivalent to the amount of MraZ used in lane 6 of panel A (lane 2). The mutant operators were incubated similarly (O_1, lane 4; O_2, lane 6; O_3, lane 8; O_4, lane 10). The corresponding DNA-only lanes are as follows: O_{WT}, lane 1; O_1, lane 3; O_2, lane 5; O_3, lane 7; O_4, lane 9. (D) Competition with unlabeled WT (O_{WT}) and mutant (O_1 to O_4) operators. MraZ-O_{WT} DNA complexes similar to those depicted in panel A, lane 6 (shown in lanes 1, 3, 5, 7, and 9), were competed with an approximately 8× molar excess of unlabeled WT (O_{WT}, lane 2) and mutant (O_1, lane 4; O_2, lane 6; O_3, lane 8; O_4, lane 10) operators.

In addition, the expression of an *mraZ-lacZ* fusion is not repressed by the overproduction of MraZR15A, in contrast to that of WT MraZ (Fig. 5D). These results indicate that the killing phenotype observed upon MraZ overproduction probably results from inappropriate regulation of gene expression because of DNA binding and, importantly, is not a nonspecific effect of protein overproduction.

Purified MraZ binds directly and specifically to its operator sites. To demonstrate directly that MraZ binds to the regulatory region near P_{mra}, we purified His_6-MraZ-GluGlu and His_6-MraZR15A-GluGlu to homogeneity and measured their binding to a 240-bp PCR-amplified DNA fragment containing the O_{WT} DRs by EMSAs. As shown in Fig. 6A, increasing concentrations of WT MraZ led to the increased formation of two stable DNA-protein complexes in the presence of the noncompetitive inhibitor poly(dI · dC) and a concomitant decrease in the amount of free DNA. In addition, unlabeled O_{WT} DNA outcompeted the binding of the highest level of MraZ (Fig. 6A, lane 7). Importantly, when WT MraZ was replaced with similar amounts of purified MraZR15A protein, no binding to O_{WT} DNA was detected (Fig. 6B), consistent with the lack of MraZR15A toxicity *in vivo*. Thus, purified WT MraZ binds specifically to O_{WT} *in vitro*, and the toxicity observed upon its overproduction is directly related to its ability to bind to its DNA site(s).

We have shown that MraZ binds to the O_{WT} operator containing three consecutive DRs and that when these DRs are mutated, the *mraZ-lacZ* fusion is derepressed. We predicted that the derepression was a direct consequence of impaired DNA binding, being affected to various degrees when the mutant operators O_1 to O_4 were used instead of O_{WT}. To test this, we added WT MraZ protein to DNA fragments with mutant operators and measured DNA binding in EMSAs. As shown in Fig. 6C and D, binding of MraZ was impaired to various degrees when the mutant operators were substituted for O_{WT}, especially when O_4 was used (Fig. 6C, lanes 9 and 10). This is consistent with the *mraZ-lacZ* fusion activities.

The results of competition assays were also consistent with the reporter fusion experiments. When an MraZ-O_{WT} complex was competed with O_{WT} or the O_1 to O_4 mutants separately, only O_{WT} successfully outcompeted the labeled DNA, as evidenced by its release from the MraZ-O_{WT} complex (Fig. 6D, lane 2). Taken together, our results suggest that MraZ represses transcription from P_{mra} and that MraZ overproduction toxicity might result, at least in part, from MraZ binding to the DRs near P_{mra} and possibly overrepression of P_{mra} (Fig. 4 and 5). This would lead to the underexpression of essential cell division genes such as *ftsL* and *ftsI* (Fig. 1A).

Evidence that MraZ may have additional targets in addition to the operator at P_{mra}. As MraZ binds to the operator site in front of its own gene and represses expression from the P_{mra} promoter, we wanted to determine how many *dcw* cluster-proximal genes are affected in their expression by MraZ binding. In addition, an assessment of whether MraZ regulates the expression of P_{mra} exclusively or whether it has a broader regulatory spectrum was also of paramount importance. We addressed these important questions by RNA-seq analysis.

We reasoned that to distinguish the effects of MraZ on gene expression most effectively, we would analyze expression data from two different stages of the cell cycle as described in Materials and Methods. This was based on the similarity of MraZ to AbrB in their DNA-binding region and the aforementioned observation that *mraW* mutant cells containing extra copies of *mraZ* have a lower than normal growth rate during early stages of growth before normal growth is resumed during later growth stages (Fig. 2B). We therefore chose two conditions for RNA-seq analysis, (i) the *mraZ* null mutant strain compared with the WT at a high cell

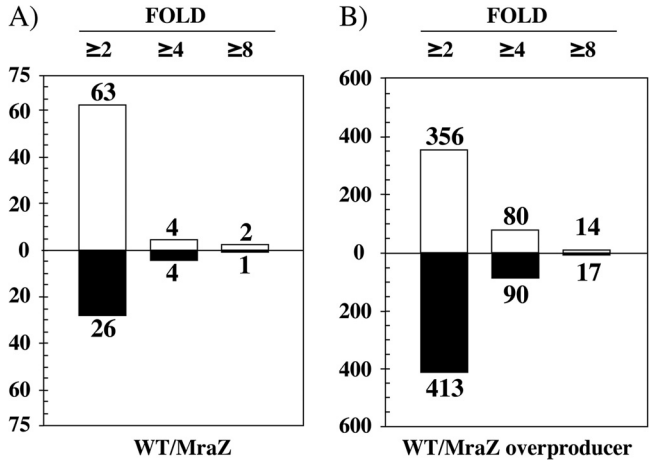

FIG 7 Gene expression analysis by RNA-seq. The numbers of genes activated (white columns) or repressed (black columns) by MraZ are shown; they were binned by the fold changes in their expression (top). These genes were selected as follows. First, only genes with an FDR of ≤0.05 were chosen; second, the cutoff for differential gene expression was set at a nonlogFC value of ≥2 (or ≥2-fold). (A) WT MG1655 and a *mraZ* mutant containing the pDSW208 vector were grown in LB to stationary phase (OD of ≥1.4). Cells were collected, and the total RNA was extracted and subjected to RNA-seq analysis. (B) WT MG1655 containing either the pDSW208 vector alone or carrying *mraZ* was grown in LB to early log phase (OD of ≤0.1) and induced with 50 μM IPTG for 30 min. Cells were collected, and total RNA was extracted and subject to RNA-seq analysis.

density and (ii) the WT strain overproducing MraZ compared with the WT in the early log phase. Overproduction of MraZ-GluGlu was confirmed by reverse transcription-PCR and immunoblotting with anti-GluGlu antibodies, similar to the data shown in Fig. 5C.

Our RNA-seq data suggested that MraZ has additional targets in *E. coli*. We found that approximately 2% of *E. coli* genes are regulated ≥2-fold by MraZ when comparing an *mraZ* null mutant to the WT parent in stationary phase. This regulation might be direct or indirect, but it is clear that MraZ can activate (Fig. 7A, white bars) or repress (Fig. 7A, black bars) transcription. A total of 69 genes were activated by MraZ, and 31 were repressed (see Table S4 in the supplemental material).

Additionally, we also found differential regulation in approximately 23% of the *E. coli* genes when MraZ is mildly overproduced in early log phase cells of the WT strain relative to WT cells containing the vector alone (Fig. 7B). Notably, the RNA levels of the first 11 genes of the *dcw* cluster are significantly decreased, as expected from repression of P_{mra} by MraZ. The genes affected are widespread throughout several functional categories, including metabolic and unknown genes.

Additional potential targets for regulation by MraZ. We then investigated the effects of the loss or excess of MraZ on specific pathways. The false-discovery rate (FDR) for the individual genes cited in this section was ≥0.05, indicating that the differential expression was statistically significant. We used functional enrichment analysis to identify pathways and functions that were biased toward differential regulation by MraZ. As the purpose of this study was to discover new potential roles for MraZ rather than validation, we set a liberal significance cutoff of 0.25 for the FDR.

When we compared the expression of genes in the WT strain with that in the *mraZ* null mutant, both grown to stationary phase, we found that the arginine catabolism pathway was transcriptionally repressed by physiological levels of MraZ (see Table S4 in the supplemental material; values in parentheses are fold changes in expression). The specific genes repressed by MraZ were *astA* (−3.5-fold), *astB* (−2.3-fold), *astC* (−4.7-fold), and *astD* (−3.2-fold) (see Table S4; highlighted in purple). The transcript levels of these genes, in general, were barely detectable at low cell density. In addition, the putrescine utilization pathway (see Table S4; highlighted in blue) was also repressed by physiological levels of MraZ under these same conditions. Those genes were *puuA* (−4.3-fold), *puuB* (−6.5-fold), *puuD* (−3.0-fold), and *puuP* (−2.4-fold); in contrast, *puuA* (+6.4-fold), *puuB* (+7.8-fold), *puuC* (+3.0-fold), *puuD* (+8.1-fold), *puuE* (+11.2-fold), and *puuR* (+4.4-fold) were activated by MraZ overproduction at low cell density. In addition, of the 69 genes activated by MraZ, 13 encode proteins involved in translation (see Table S4; highlighted in yellow).

In contrast to the activator role suggested for MraZ early in log phase (see below), the fatty acid (FA) degradation operon *fadBA* and the monocistronic genes *fadD* and *fadE* were repressed ~2-fold by MraZ. We attribute this seeming paradox to the possibility that additional factors superimpose regulation on these genes. For example, *fadB* and *fadE* are both repressed by FadR in the absence of long-chain FAs and by ArcA-P under anaerobic growth conditions (54). MraZ activates the expression of both *fadB* and *fadE* when overexpressed early in the highly aerobic log phase, when ArcA is not phosphorylated and is inactive as a repressor. In stationary phase, however, ArcA-P represses both *fadB* and *fadE*, which could prevent activation by MraZ.

MraZ repression of P_{mra} expression, as inferred from our data (Fig. 4 to 6), suggests that MraZ can potentially regulate genes for cell division and PG metabolism. In addition to the synthetic effects of combining *ftsZ* and *min* mutants with excess MraZ described above, we found two sets of genes involved in cell division that were repressed to various extents by MraZ overproduction during growth in early logarithmic phase. The first set includes the *dcw* cluster genes downstream from *mraZ*. These are, in order from upstream to downstream, *ftsL* (−3.0-fold), *ftsI* (−3.5-fold), *murE* (−3.5-fold), *murF* (−3.3-fold), *mraY* (−3.4-fold), *murD* (−2.9-fold), *ftsW* (−2.8-fold), *murG* (−2.4-fold), and *murC* (−2.2-fold). The *mraW* gene (−3.3-fold) was also repressed, but the FDR was >0.05. The *ddlB*, *ftsQ*, *ftsA*, and *ftsZ* genes downstream of *murC* were not affected. Thus, consistent with previous reports (11, 31) the P_{mra} transcript is likely to encompass the first 11 genes in the *dcw* cluster, extending from *mraZ* to *murC* but not to *ddlB* (Fig. 1A). The second set of MraZ-repressed genes includes cell division genes unlinked to the *dcw* cluster, including *amiA* (−7.1-fold), *cedA* (−3.6-fold), *ftsB* (−6.9-fold), *mltF* (−2.4-fold), *mltD* (−2.3-fold), *mrdA* (−3.3-fold), *pbpC* (−2.4-fold), *ycfS* (−3.7-fold), and *zapB* (−2.0-fold).

Metabolic genes were also regulated by MraZ overproduction. The trichloroacetic acid (TCA) cycle was activated by MraZ overproduction early in logarithmic phase; *acnA* (+3.0-fold), *acnB* (+4.5-fold), *gltA* (+5.2-fold), *mdh* (+4.5-fold), *sdhA* (+4.2-fold), *sdhB* (+3.1-fold), *sdhC* (+2.8-fold), *sdhD* (+4.1-fold), *sucA* (+3.3-fold), *sucB* (+3.9-fold), *sucC* (+4.1-fold), and *sucD* (+3.2-fold) were all activated. In addition, the FA oxidation pathway was also activated by MraZ overproduction. The representative genes from this pathway are *aidB* (+2.9-fold), *fadB* (+5.1-fold), and *fadE* (+2.6-fold).

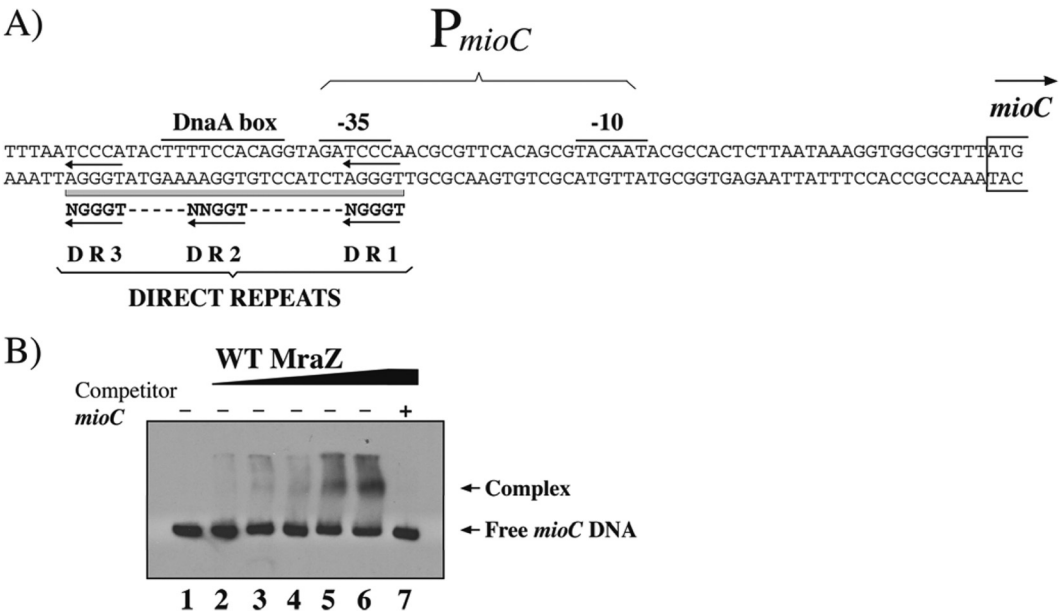

FIG 8 Binding of MraZ to the *mioC* regulatory region. (A) The DNA sequence of the *mioC* regulatory region is shown, including P_{mioC} and the DnaA box (56). DR1 to DR3 represent the three DRs separated by 8- and 5-nt spacer regions. DR2 is 1 nt from the consensus TGGGN. (B) Binding of increasing concentrations of WT MraZ to biotinylated *mioC*. About 0.3 pmol of a biotinylated double-stranded 238-bp fragment containing the *mioC* regulatory region was incubated with 3.2 (lane 2), 6.4 (lane 3), 10.7 (lane 4), 32 (lane 5), or 96 (lane 6) pmol of MraZ protein. The components in lane 7 were the same as those in lane 6, with the addition of an approximately 10× molar excess of unlabeled *mioC* DNA. Lane 1 is biotinylated *mioC* DNA only.

MraZ binds to the *mioC* regulatory region. To validate the RNA-seq data further, we inspected differentially expressed genes by scanning their regulatory regions for the presence of a putative MraZ-binding DNA sequence. Since no other gene in the genome contains the same number of DRs with the same spacing distribution as that in front of *mraZ*, we searched for any multiple DR T-G-G-G-N sequences separated by variable spacing regions. One gene selected this way was *mioC*, which, according to the RNA-seq data, is negatively regulated by MraZ overproduction by as much as 12-fold during early log phase. Transcription through *mioC* has been reported to affect initiation of chromosome replication (55, 56), although its effect might be more prevalent under suboptimal growth conditions (57). The regulatory region of *mioC* is depicted in Fig. 8A. We defined three MraZ consensus DRs as DR1, DR2 and DR3, where DR2 contains one mismatch.

We then used EMSAs to test whether MraZ binds directly to this region. Purified MraZ bound to a 238-bp fragment containing the *mioC* regulatory region, forming one complex (Fig. 8B). The MraZ-*mioC* DNA complex formed less readily than the two complexes observed for MraZ-P_{mra}-*mraZ* DNA (Fig. 6A), most likely because of lower binding affinity for *mioC* than for P_{mra}-*mraZ*. Nevertheless, addition of unlabeled competitor *mioC* DNA at an approximately ≥10-fold molar excess displaced MraZ from MraZ-*mioC* DNA complexes, suggesting that MraZ binds to the regulatory region of *mioC* specifically.

The *mioC* gene encodes a flavodoxin involved in biotin synthesis, and it has been reported that cell division is retarded in biotin-deficient medium (58). To test if excess MraZ might result in the lack of this flavodoxin and contribute to the lethality of MraZ overproduction, we overproduced the MioC protein from a compatible plasmid while overproducing MraZ and found that cells were still killed by MraZ overproduction (data not shown). This argues against the possibility that the lack of the MioC protein contributes significantly to MraZ-mediated killing, and in favor of possible effects of *mioC* transcription on *oriC*.

DISCUSSION

In this study, we set out to investigate the cellular role of MraZ. Our findings support the idea that *mraZ* and its downstream neighbor gene, *mraW*, are evolutionarily conserved but nonessential (40, 43–45). This apparent contradiction suggests that there is stringent selection acting on these two genes (59). We tested for *mraZ* and *mraW* essentiality by assaying both aerobic and anaerobic growth in rich and minimal media, as performed by others for alternative genes (60). In addition, we tested sensitivity to different classes of antibiotics and survival in stationary phase. Although we observed no effects with many antibiotics, *mraZ* null mutants were more resistant to trimethoprim than the WT strain and *mraW* null mutants were more sensitive. This is consistent with our other evidence suggesting that MraW antagonizes MraZ function, and it is the first phenotype reported for the loss of *mraZ*. Trimethoprim inhibits DHFR and one-carbon metabolism, which might be involved in the function of the MraW methylase, potentially impacting MraZ activity. The significance of this will be investigated further.

As co-overproduction of MraW protects cells from the effects of MraZ overproduction *in vivo* and *mraZ* and *mraW* are usually a tightly linked gene pair, it is reasonable to assume that this effect is direct, although additional data are needed. How could MraW be affecting MraZ? One possibility is that MraZ could be inhibited by an MraW-mediated posttranslational modification. Another is that direct MraW binding to MraZ could inhibit MraZ activity, similar to MazE inhibition of the MazF toxin (61). Alternatively, MraW might somehow decrease cellular levels of the MraZ pro-

tein. Any of these scenarios might result in more *mraW* gene expression because of the loss of MraZ repression at P_{mra}, which would induce a positive feedback loop. Irrespective of the mechanism, our results suggest that MraZ and MraW regulate each other and argue that MraW is above MraZ in the putative regulatory cascade.

What might be the molecular mechanism of MraZ transcriptional regulation? We have observed high-molecular-weight MraZ multimers in denaturing SDS gels with purified MraZ-GluGlu (data not shown), consistent with the reported dodecameric structure of *E. coli* MraZ in solution (18). Dodecameric transcriptional regulators from bacteria have rarely been reported. Three known examples adopting this quaternary structure are anti-TRAP (*trp* RNA-binding attenuation protein) in *Bacillus* species (62), the YjiE hypochlorite-specific transcription factor (63), and the Dps DNA condensation protein (64), the latter two of which are both from *E. coli*. If MraZ indeed binds to DNA as a dodecamer, it might wrap the DNA around its toroidal structure similar to the *E. coli* transcriptional repressor RcnR (65) and DNA gyrase (66). In addition, as a dodecamer, six times more protein would be necessary for DNA binding than for a dimer, which could explain the relatively high MraZ concentration needed to detect band shifts in our EMSAs. Alternatively, MraZ may assemble into polymers of dimers similar to MazE (67) or ArcA-P, the latter being able to occupy two, three, and even four consecutive DR sequences separated by variable spacer regions, all located on one side of the helix (68). In our experiments, the existence of two distinct MraZ-O_{WT} complexes would be consistent with the binding of two MraZ dimers to the operator site.

The three TGGGN repeats in the *mraZ* O_{WT} operator are separated by 5-nt spacers, indicating that the repeats face the same side of the DNA helix; similarly, AbrB also binds to residues located on one side of the helix (50). Thus far, we have not been able to define a consensus DNA-binding sequence for MraZ, as the number and distribution of DRs are highly variable in all of the genes examined, similarly to AbrB DNA-binding regions (15, 69). AbrB, which integrates environmental and metabolic information to minimize inappropriate gene expression during log phase (70), shows similarity to MraZ in its "looped-hinge helix fold" DNA-binding domain. Therefore, MraZ might use a similar strategy for DNA recognition, allowing it to bind unrelated DNA sequences in a specific manner. It may even act like AbrB, with higher or lower activity, depending on the growth phase.

The toxicity from MraZ overproduction was more pronounced in minimal medium. When *E. coli* cells grow in minimal glycerol medium, they exhibit a carbon stress response (71). Cells readjust their metabolism by using the transcriptional regulators Cra (FruR), which, among its other functions, downregulates the TCA cycle (72); the CRP-cyclic AMP complex; and the ArcBA two-component system. Our RNA-seq data showed that MraZ overproduction represses *cra* transcription by 4.4-fold, either directly or indirectly, and as would be expected, upregulates TCA cycle genes. Thus, altered expression of TCA cycle genes, which has been shown to involve other regulators (73), might be partly responsible for the sensitivity to MraZ overproduction under these particular growth conditions.

MraZ, at physiological levels, has the potential to autoregulate its expression and that of the first 11 genes in the *dcw* cluster, including *mraW*, by binding to the O_{WT} operator at P_{mra}. Such repression by MraZ might limit the amount of some essential cell division and/or PG biosynthesis proteins, and this is the likely cause of cell division inhibition after the overproduction of MraZ. Despite this phenotype, an *mraZ* null mutant shows no significant changes in *dcw* gene expression, at least in stationary phase. This suggests that MraZ may be more active as a repressor during stress conditions or other stages of growth, and/or MraZ function is redundant with another transcriptional regulator.

Although they do not affect *dcw* transcription in stationary phase, it is important to emphasize that physiological levels of MraZ do repress the transcription of arginine and polyamine catabolism, the *ast* and *puu* genes, respectively, and activate other genes encoding proteins involved in translation. This indicates that increases in polyamine concentration and some regulation of translation in stationary phase might be a consequence of MraZ activity. These differences in gene expression between an *mraZ* null mutant and the isogenic WT parent suggest that MraZ might have a role in cell adaptation or survival in suboptimal environments or under suboptimal growth conditions, as has been proposed for the MazEF toxin-antitoxin system (74, 75).

In summary, here we show that MraZ, the product of the highly conserved *mraZ* gene, acts as a transcriptional regulator in *E. coli*. By binding to a DNA sequence organized with different combinations of TGGGN DRs located immediately downstream from the P_{mra} promoter, MraZ represses its own expression and that of the 10 subsequent genes in the proximal part of the *dcw* cluster. In addition, overproduction of MraZ inhibits cell division, but co-overproduction with MraW suppresses MraZ toxicity, suggesting that MraZ and MraW may have antagonistic functions. Finally, several lines of evidence, including MraZ localization throughout the nucleoid, activation or repression of multiple genes by RNA-seq, and *in vitro* binding to the *mioC* gene near *oriC*, suggest that MraZ may also regulate the expression of genes outside the *dcw* cluster and perhaps influence other cell cycle functions.

ACKNOWLEDGMENTS

We thank members of the Margolin laboratory, David Bates, and George Phillips for helpful discussions; Christopher C. Overall for help with bioinformatic analysis; and Audrey Wanger for generously providing antibiotic Etest strips.

A portion of the research described here was performed with EMSL, a national scientific user facility sponsored by the Department of Energy's Office of Biological and Environmental Research and located at Pacific Northwest National Laboratory. The remainder of the research was supported by NIH grant GM61074 to W.M.

REFERENCES

1. **Blasco B, Pisabarro AG, de Pedro MA.** 1988. Peptidoglycan biosynthesis in stationary-phase cells of *Escherichia coli*. J. Bacteriol. **170:**5224–5228.
2. **Clark DJ.** 1968. The regulation of DNA replication and cell division in *E. coli* B-r. Cold Spring Harbor Symp. Quant. Biol. **33:**823–838. http://dx.doi.org/10.1101/SQB.1968.033.01.094.
3. **Lee YS, Han JS, Jeon Y, Hwang DS.** 2001. The *arc* two-component signal transduction system inhibits in vitro *Escherichia coli* chromosomal initiation. J. Biol. Chem. **276:**9917–9923. http://dx.doi.org/10.1074/jbc.M008629200.
4. **Loeb A, McGrath BE, Navre JM, Pierucci O.** 1978. Cell division during nutritional upshifts of *Escherichia coli*. J. Bacteriol. **136:**631–637.
5. **Walker HH, Winslow CE, Mooney MG.** 1934. Bacterial cell metabolism under anaerobic conditions. J. Gen. Physiol. **17:**349–357. http://dx.doi.org/10.1085/jgp.17.3.349.
6. **Chen S, Jancrick J, Yokota H, Kim R, Kim SH.** 2004. Crystal structure of a protein associated with cell division from *Mycoplasma pneumoniae*

(GI: 13508053): a novel fold with a conserved sequence motif. Proteins **55:**785–791. http://dx.doi.org/10.1002/prot.10593.
7. **Mingorance J, Tamames J, Vicente M.** 2004. Genomic channeling in bacterial cell division. J. Mol. Recognit. **17:**481–487. http://dx.doi.org/10.1002/jmr.718.
8. **Tamames J, Gonzalez-Moreno M, Mingorance J, Valencia A, Vicente M.** 2001. Bringing gene order into bacterial shape. Trends Genet. **17:**124–126. http://dx.doi.org/10.1016/S0168-9525(00)02212-5.
9. **Szklarczyk D, Franceschini A, Kuhn M, Simonovic M, Roth A, Minguez P, Doerks T, Stark M, Muller J, Bork P, Jensen LJ, von Mering C.** 2010. The STRING database in 2011: functional interaction networks of proteins, globally integrated and scored. Nucleic Acids Res. **39:**D561–D568. http://dx.doi.org/10.1093/nar/gkq973.
10. **Tatusov RL, Koonin EV, Lipman DJ.** 1997. A genomic perspective on protein families. Science **278:**631–637. http://dx.doi.org/10.1126/science.278.5338.631.
11. **Hara H, Yasuda S, Horiuchi K, Park JT.** 1997. A promoter for the first nine genes of the *Escherichia coli mra* cluster of cell division and cell envelope biosynthesis genes, including *ftsI* and *ftsW*. J. Bacteriol. **179:**5802–5811.
12. **Wang S, Arends SJ, Weiss DS, Newman EB.** 2005. A deficiency in *S*-adenosylmethionine synthetase interrupts assembly of the septal ring in *Escherichia coli* K-12. Mol. Microbiol. **58:**791–799. http://dx.doi.org/10.1111/j.1365-2958.2005.04864.x.
13. **Alarcon F, Ribeiro de Vasconcelos AT, Yim L, Zaha A.** 2007. Genes involved in cell division in mycoplasmas. Genet. Mol. Biol. **30:**174–181. http://dx.doi.org/10.1590/S1415-47572007000200003.
14. **Bobay BG, Andreeva A, Mueller GA, Cavanagh J, Murzin AG.** 2005. Revised structure of the AbrB N-terminal domain unifies a diverse superfamily of putative DNA-binding proteins. FEBS Lett. **579:**5669–5674. http://dx.doi.org/10.1016/j.febslet.2005.09.045.
15. **Vaughn JL, Feher VA, Bracken C, Cavanagh J.** 2001. The DNA-binding domain in the *Bacillus subtilis* transition-state regulator AbrB employs significant motion for promiscuous DNA recognition. J. Mol. Biol. **305:**429–439. http://dx.doi.org/10.1006/jmbi.2000.4305.
16. **Loris R, Marianovsky I, Lah J, Laeremans T, Engelberg-Kulka H, Glaser G, Muyldermans S, Wyns L.** 2003. Crystal structure of the intrinsically flexible addiction antidote MazE. J. Biol. Chem. **278:**28252–28257. http://dx.doi.org/10.1074/jbc.M302336200.
17. **Hsu CH, Wang AH.** 2011. The DNA-recognition fold of Sso7c4 suggests a new member of SpoVT-AbrB superfamily from archaea. Nucleic Acids Res. **39:**6764–6774. http://dx.doi.org/10.1093/nar/gkr283.
18. **Adams MA, Udell CM, Pal GP, Jia Z.** 2005. MraZ from *Escherichia coli*: cloning, purification, crystallization and preliminary X-ray analysis. Acta Crystallogr. Sect. F Struct. Biol. Cryst. Commun. **61:**378–380. http://dx.doi.org/10.1107/S1744309105007657.
19. **Miller DJ, Ouellette N, Evdokimova E, Savchenko A, Edwards A, Anderson WF.** 2003. Crystal complexes of a predicted *S*-adenosylmethionine-dependent methyltransferase reveal a typical AdoMet binding domain and a substrate recognition domain. Protein Sci. **12:**1432–1442. http://dx.doi.org/10.1110/ps.0302403.
20. **Sergiev PV, Golovina AY, Sergeeva OV, Osterman IA, Nesterchuk MV, Bogdanov AA, Dontsova OA.** 2012. How much can we learn about the function of bacterial rRNA modification by mining large-scale experimental datasets? Nucleic Acids Res. **40:**5694–5705. http://dx.doi.org/10.1093/nar/gks219.
21. **Kimura S, Suzuki T.** 2009. Fine-tuning of the ribosomal decoding center by conserved methyl-modifications in the *Escherichia coli* 16S rRNA. Nucleic Acids Res. **38:**1341–1352. http://dx.doi.org/10.1093/nar/gkp1073.
22. **Carrión M, Gomez MJ, Merchante-Schubert R, Dongarra S, Ayala JA.** 1999. *mraW*, an essential gene at the *dcw* cluster of *Escherichia coli* codes for a cytoplasmic protein with methyltransferase activity. Biochimie **81:**879–888. http://dx.doi.org/10.1016/S0300-9084(99)00208-4.
23. **Wei Y, Zhang H, Gao ZQ, Wang WJ, Shtykova EV, Xu JH, Liu QS, Dong YH.** 2012. Crystal and solution structures of methyltransferase RsmH provide basis for methylation of C1402 in 16S rRNA. J. Struct. Biol. **179:**29–40. http://dx.doi.org/10.1016/j.jsb.2012.04.011.
24. **Dewar SJ, Dorazi R.** 2000. Control of division gene expression in *Escherichia coli*. FEMS Microbiol. Lett. **187:**1–7. http://dx.doi.org/10.1111/j.1574-6968.2000.tb09127.x.
25. **Vicente M, Gomez MJ, Ayala JA.** 1998. Regulation of transcription of cell division genes in the *Escherichia coli dcw* cluster. Cell. Mol. Life Sci. **54:**317–324. http://dx.doi.org/10.1007/s000180050158.
26. **Vicente M, Errington J.** 1996. Structure, function and controls in microbial division. Mol. Microbiol. **20:**1–7. http://dx.doi.org/10.1111/j.1365-2958.1996.tb02482.x.
27. **Sitnikov DM, Schineller JB, Baldwin TO.** 1996. Control of cell division in *Escherichia coli*: regulation of transcription of *ftsQA* involves both *rpoS* and SdiA-mediated autoinduction. Proc. Natl. Acad. Sci. U. S. A. **93:**336–341. http://dx.doi.org/10.1073/pnas.93.1.336.
28. **Cam K, Rome G, Krisch HM, Bouche JP.** 1996. RNase E processing of essential cell division genes mRNA in *Escherichia coli*. Nucleic Acids Res. **24:**3065–3070. http://dx.doi.org/10.1093/nar/24.15.3065.
29. **Selinger DW, Saxena RM, Cheung KJ, Church GM, Rosenow C.** 2003. Global RNA half-life analysis in *Escherichia coli* reveals positional patterns of transcript degradation. Genome Res. **13:**216–223. http://dx.doi.org/10.1101/gr.912603.
30. **de la Fuente A, Palacios P, Vicente M.** 2001. Transcription of the *Escherichia coli dcw* cluster: evidence for distal upstream transcripts being involved in the expression of the downstream *ftsZ* gene. Biochimie **83:**109–115. http://dx.doi.org/10.1016/S0300-9084(00)01212-8.
31. **Mengin-Lecreulx D, Ayala J, Bouhss A, van Heijenoort J, Parquet C, Hara H.** 1998. Contribution of the P_{mra} promoter to expression of genes in the *Escherichia coli mra* cluster of cell envelope biosynthesis and cell division genes. J. Bacteriol. **180:**4406–4412.
32. **Flärdh K, Palacios P, Vicente M.** 1998. Cell division genes *ftsQAZ* in *Escherichia coli* require distant *cis*-acting signals upstream of *ddlB* for full expression. Mol. Microbiol. **30:**305–315. http://dx.doi.org/10.1046/j.1365-2958.1998.01064.x.
33. **Dai K, Lutkenhaus J.** 1991. *ftsZ* is an essential cell division gene in *Escherichia coli*. J. Bacteriol. **173:**3500–3506.
34. **Göhler A-K, Kokpinar O, Schmidt-Heck W, Geffers R, Guthke R, Rinas U, Schuster S, Jahreis K, Kaleta C.** 2011. More than just a metabolic regulator—elucidation and validation of new targets of PdhR in *Escherichia coli*. BMC Syst. Biol. **5:**197–208. http://dx.doi.org/10.1186/1752-0509-5-197.
35. **Silhavy TJ, Berman ML, Enquist LW.** 1984. Experiments with gene fusions. Cold Spring Harbor Laboratory, Cold Spring Harbor, NY.
36. **Robinson MD, McCarthy DJ, Smyth GK.** 2010. edgeR: a Bioconductor package for differential expression analysis of digital gene expression data. Bioinformatics **26:**139–140. http://dx.doi.org/10.1093/bioinformatics/btp616.
37. **Subramanian A, Tamayo P, Mootha VK, Mukherjee S, Ebert BL, Gillette MA, Paulovich A, Pomeroy SL, Golub TR, Lander ES, Mesirov JP.** 2005. Gene set enrichment analysis: a knowledge-based approach for interpreting genome-wide expression profiles. Proc. Natl. Acad. Sci. U. S. A. **102:**15545–15550. http://dx.doi.org/10.1073/pnas.0506580102.
38. **Tai TN, Havelka WA, Kaplan S.** 1988. A broad-host-range vector system for cloning and translational *lacZ* fusion analysis. Plasmid **19:**175–188. http://dx.doi.org/10.1016/0147-619X(88)90037-6.
39. **Eraso JM, Kaplan S.** 2002. Redox flow as an instrument of gene regulation. Methods Enzymol. **348:**216–229. http://dx.doi.org/10.1016/S0076-6879(02)48640-5.
40. **Merlin C, McAteer S, Masters M.** 2002. Tools for characterization of *Escherichia coli* genes of unknown function. J. Bacteriol. **184:**4573–4581. http://dx.doi.org/10.1128/JB.184.16.4573-4581.2002.
41. **Eraso JM, Kaplan S.** 2009. Regulation of gene expression by PrrA in *Rhodobacter sphaeroides* 2.4.1: role of polyamines and DNA topology. J. Bacteriol. **191:**4341–4352. http://dx.doi.org/10.1128/JB.00243-09.
42. **Grussenmeyer T, Scheidtmann KH, Hutchinson MA, Eckhart W, Walter G.** 1985. Complexes of polyoma virus medium T antigen and cellular proteins. Proc. Natl. Acad. Sci. U. S. A. **82:**7952–7954. http://dx.doi.org/10.1073/pnas.82.23.7952.
43. **Baba T, Ara T, Hasegawa M, Takai Y, Okumura Y, Baba M, Datsenko KA, Tomita M, Wanner BL, Mori H.** 2006. Construction of *Escherichia coli* K-12 in-frame, single-gene knockout mutants: the Keio collection. Mol. Syst. Biol. **2:**2006.0008. http://dx.doi.org/10.1038/msb4100050.
44. **Dassain M, Leroy A, Colosetti L, Carole S, Bouche JP.** 1999. A new essential gene of the 'minimal genome' affecting cell division. Biochimie **81:**889–895. http://dx.doi.org/10.1016/S0300-9084(99)00207-2.
45. **Daniel RA, Williams AM, Errington J.** 1996. A complex four-gene operon containing essential cell division gene *pbpB* in *Bacillus subtilis*. J. Bacteriol. **178:**2343–2350.
46. **Dandekar T, Snel B, Huynen M, Bork P.** 1998. Conservation of gene order: a fingerprint of proteins that physically interact. Trends Biochem. Sci. **23:**324–328. http://dx.doi.org/10.1016/S0968-0004(98)01274-2.

47. **RayChaudhuri D, Park JT.** 1992. *Escherichia coli* cell-division gene *ftsZ* encodes a novel GTP-binding protein. Nature **359:**251–254. http://dx.doi.org/10.1038/359251a0.
48. **Stricker J, Maddox P, Salmon ED, Erickson HP.** 2002. Rapid assembly dynamics of the *Escherichia coli* FtsZ-ring demonstrated by fluorescence recovery after photobleaching. Proc. Natl. Acad.Sci. U. S. A. **99:**3171–3175. http://dx.doi.org/10.1073/pnas.052595099.
49. **Yu X-C, Margolin W.** 1999. FtsZ ring clusters in *min* and partition mutants: role of both the Min system and the nucleoid in regulating FtsZ ring localization. Mol. Microbiol. **32:**315–326. http://dx.doi.org/10.1046/j.1365-2958.1999.01351.x.
50. **Strauch MA, Perego M, Burbulys D, Hoch JA.** 1989. The transition state transcription regulator AbrB of *Bacillus subtilis* is autoregulated during vegetative growth. Mol. Microbiol. **3:**1203–1209. http://dx.doi.org/10.1111/j.1365-2958.1989.tb00270.x.
51. **Zhang J, Zhang Y, Inouye M.** 2003. Characterization of the interactions within the *mazEF* addiction module of *Escherichia coli*. J. Biol. Chem. **278:**32300–32306. http://dx.doi.org/10.1074/jbc.M304767200.
52. **McClure WR, Hawley DK, Youderian P, Susskind MM.** 1983. DNA determinants of promoter selectivity in *Escherichia coli*. Cold Spring Harbor Symp. Quant. Biol. **47**(Pt 1):477–481. http://dx.doi.org/10.1101/SQB.1983.047.01.057.
53. **Chumsakul O, Takahashi H, Oshima T, Hishimoto T, Kanaya S, Ogasawara N, Ishikawa S.** 2011. Genome-wide binding profiles of the *Bacillus subtilis* transition state regulator AbrB and its homolog Abh reveals their interactive role in transcriptional regulation. Nucleic Acids Res. **39:**414–428. http://dx.doi.org/10.1093/nar/gkq780.
54. **Cho B-K, Knight EM, Palsson BO.** 2006. Transcriptional regulation of the *fad* regulon genes of *Escherichia coli* by ArcA. Microbiology **152:**2207–2219. http://dx.doi.org/10.1099/mic.0.28912-0.
55. **Ogawa T, Okazaki T.** 1994. Cell cycle-dependent transcription from the *gid* and *mioC* promoters of *Escherichia coli*. J. Bacteriol. **176:**1609–1615.
56. **Stuitje AR, de Wind N, van der Spek JC, Pors TH, Meijer M.** 1986. Dissection of promoter sequences involved in transcriptional activation of the *Escherichia coli* replication origin. Nucleic Acids Res. **14:**2333–2344. http://dx.doi.org/10.1093/nar/14.5.2333.
57. **Bates DB, Boye E, Asai T, Kogoma T.** 1997. The absence of effect of *gid* or *mioC* transcription on the initiation of chromosomal replication in *Escherichia coli*. Proc. Natl. Acad. Sci. U. S. A. **94:**12497–12502. http://dx.doi.org/10.1073/pnas.94.23.12497.
58. **Summers JW, Wyss O.** 1967. Biotin-deficient growth of *Bacillus polymyxa*. J. Bacteriol. **94:**1908–1914.
59. **Jordan IK, Rogozin IB, Wolf YI, Koonin EV.** 2002. Essential genes are more evolutionarily conserved than are nonessential genes in bacteria. Genome Res. **12:**962–968. http://dx.doi.org/10.1101/gr.87702.
60. **Tong X, Campbell JW, Balazsi G, Kay KA, Wanner BL, Gerdes SY, Oltvai ZN.** 2004. Genome-scale identification of conditionally essential genes in *E. coli* by DNA microarrays. Biochem. Biophys. Res. Commun. **322:**347–354. http://dx.doi.org/10.1016/j.bbrc.2004.07.110.
61. **Zhang Y, Zhang J, Hoeflich KP, Ikura M, Qing G, Inouye M.** 2003. MazF cleaves cellular mRNAs specifically at ACA to block protein synthesis in *Escherichia coli*. Mol. Cell **12:**913–923. http://dx.doi.org/10.1016/S1097-2765(03)00402-7.
62. **Snyder D, Lary J, Chen Y, Gollnick P, Cole JL.** 2004. Interaction of the *trp* RNA-binding attenuation protein (TRAP) with anti-TRAP. J. Mol. Biol. **338:**669–682. http://dx.doi.org/10.1016/j.jmb.2004.03.030.
63. **Gebendorfer KM, Drazic A, Le Y, Gundlach J, Bepperling A, Kastenmuller A, Ganzinger KA, Braun N, Franzmann TM, Winter J.** 2012. Identification of a hypochlorite-specific transcription factor from *Escherichia coli*. J. Biol. Chem. **287:**6892–6903. http://dx.doi.org/10.1074/jbc.M111.287219.
64. **Grant RA, Filman DJ, Finkel SE, Kolter R, Hogle JM.** 1998. The crystal structure of Dps, a ferritin homolog that binds and protects DNA. Nat. Struct. Biol. **5:**294–303. http://dx.doi.org/10.1038/nsb0498-294.
65. **Iwig JS, Chivers PT.** 2009. DNA recognition and wrapping by *Escherichia coli* RcnR. J. Mol. Biol. **393:**514–526. http://dx.doi.org/10.1016/j.jmb.2009.08.038.
66. **Orphanides G, Maxwell A.** 1994. Evidence for a conformational change in the DNA gyrase-DNA complex from hydroxyl radical footprinting. Nucleic Acids Res. **22:**1567–1575. http://dx.doi.org/10.1093/nar/22.9.1567.
67. **Lah J, Marianovsky I, Glaser G, Engelberg-Kulka H, Kinne J, Wyns L, Loris R.** 2003. Recognition of the intrinsically flexible addiction antidote MazE by a dromedary single domain antibody fragment. Structure, thermodynamics of binding, stability, and influence on interactions with DNA. J. Biol. Chem. **278:**14101–14111. http://dx.doi.org/10.1074/jbc.M209855200.
68. **Park DM, Akhtar MS, Ansari AZ, Landick R, Kiley PJ.** 2013. The bacterial response regulator ArcA uses a diverse binding site architecture to regulate carbon oxidation globally. PLoS Genet. **9:**e1003839. http://dx.doi.org/10.1371/journal.pgen.1003839.
69. **Vaughn JL, Feher V, Naylor S, Strauch MA, Cavanagh J.** 2000. Novel DNA binding domain and genetic regulation model of *Bacillus subtilis* transition state regulator *abrB*. Nat. Struct. Biol. **7:**1139–1146. http://dx.doi.org/10.1038/81999.
70. **Strauch MA, Hoch JA.** 1993. Transition-state regulators: sentinels of *Bacillus subtilis* post-exponential gene expression. Mol. Microbiol. **7:**337–342. http://dx.doi.org/10.1111/j.1365-2958.1993.tb01125.x.
71. **Martínez-Gómez K, Flores N, Castaneda HM, Martínez-Batallar G, Hernandez-Chavez G, Ramirez OT, Gosset G, Encarnacion S, Bolivar F.** 2012. New insights into *Escherichia coli* metabolism: carbon scavenging, acetate metabolism and carbon recycling responses during growth on glycerol. Microb. Cell Fact. **11:**46. http://dx.doi.org/10.1186/1475-2859-11-46.
72. **Shimada T, Yamamoto K, Ishihama A.** 2011. Novel members of the Cra regulon involved in carbon metabolism in *Escherichia coli*. J. Bacteriol. **193:**649–659. http://dx.doi.org/10.1128/JB.01214-10.
73. **Perrenoud A, Sauer U.** 2005. Impact of global transcriptional regulation by ArcA, ArcB, Cra, Crp, Cya, Fnr, and Mlc on glucose catabolism in *Escherichia coli*. J. Bacteriol. **187:**3171–3179. http://dx.doi.org/10.1128/JB.187.9.3171-3179.2005.
74. **Hazan R, Sat B, Engelberg-Kulka H.** 2004. *Escherichia coli mazEF*-mediated cell death is triggered by various stressful conditions. J. Bacteriol. **186:**3663–3669. http://dx.doi.org/10.1128/JB.186.11.3663-3669.2004.
75. **Ramisetty BC, Natarajan B, Santhosh RS.** 25 June 2013. *mazEF*-mediated programmed cell death in bacteria: "what is this?" Crit. Rev. Microbiol. (Epub ahead of print.) http://dx.doi.org/10.3109/1040841X.2013.804030.
76. **Sambrook J, Fritsch EF, Maniatis T.** 1989. Molecular cloning: a laboratory manual, 2nd ed. Cold Spring Harbor Laboratory Press, Cold Spring Harbor, NY.
77. **Eraso JM, Kaplan S.** 1994. *prrA*, a putative response regulator involved in oxygen regulation of photosynthesis gene expression in *Rhodobacter sphaeroides*. J. Bacteriol. **176:**32–43.
78. **Blattner FR, Plunkett G, III, Bloch CA, Perna NT, Burland V, Riley M, Collado-Vides J, Glasner JD, Rode CK, Mayhew GF, Gregor J, Davis NW, Kirkpatrick HA, Goeden MA, Rose DJ, Mau B, Shao Y.** 1997. The complete genome sequence of *Escherichia coli* K-12. Science **277:**1453–1462. http://dx.doi.org/10.1126/science.277.5331.1453.
79. **Geissler B, Shiomi D, Margolin W.** 2007. The *ftsA** gain-of-function allele of *Escherichia coli* and its effects on the stability and dynamics of the Z ring. Microbiology **153:**814–825. http://dx.doi.org/10.1099/mic.0.2006/001834-0.
80. **Guzman L-M, Belin D, Carson MJ, Beckwith J.** 1995. Tight regulation, modulation, and high-level expression by vectors containing the arabinose P_{BAD} promoter. J. Bacteriol. **177:**4121–4130.
81. **Weiss DS, Chen JC, Ghigo JM, Boyd D, Beckwith J.** 1999. Localization of FtsI (PBP3) to the septal ring requires its membrane anchor, the Z ring, FtsA, FtsQ, and FtsL. J. Bacteriol. **181:**508–520.
82. **Keen NT, Tamaki S, Kobayashi D, Trollinger D.** 1988. Improved broad-host-range plasmids for DNA cloning in Gram-negative bacteria. Gene **70:**191–197. http://dx.doi.org/10.1016/0378-1119(88)90117-5.